Published in final edited form as:

Circ Res. 2023 February 17; 132(4): 432–448. doi:10.1161/CIRCRESAHA.122.322096.

Homeostatic, Non-Canonical Role of Macrophage Elastase in Vascular Integrity

Mani Salarian[1,2,*], **Mean Ghim**[1,2,*], **Jakub Toczek**[1,2], **Jinah Han**[1,2], **Dar Weiss**[3], **Bart Spronck**[3], **Abhay B. Ramachandra**[3], **Jae-Joon Jung**[1,2], **Gunjan Kukreja**[1,2], **Jiasheng Zhang**[1,2], **Deaneira Lakheram**[4], **Sung-Kwon Kim**[4], **Jay D. Humphrey**[3,5], **Mehran M. Sadeghi**[1,2]

[1]Section of Cardiovascular Medicine and Cardiovascular Research Center, Yale School of Medicine, New Haven, CT, USA.

[2]VA Connecticut Healthcare System, West Haven, CT, USA.

[3]Department of Biomedical Engineering, Yale University, New Haven, CT, USA.

[4]Alexion Pharmaceuticals, New Haven, CT, USA

[5]Vascular Biology and Therapeutics Program, Yale School of Medicine, New Haven, CT, USA.

Abstract

Background—Matrix metalloproteinase (MMP)-12 is highly expressed in abdominal aortic aneurysms (AAAs) and its elastolytic function has been implicated in the pathogenesis. This concept is challenged, however, by conflicting data. Here, we sought to revisit the role of MMP-12 in AAA.

Corresponding Author: Mehran M. Sadeghi, M.D., Professor of Medicine (Cardiology), Yale School of Medicine, 300 George Street, Room 770G, New Haven, CT 06511, USA, Phone: 203-737 6954, Fax: 203-937 3884, mehran.sadeghi@yale.edu.

*Equal contribution

Author Contributions.

MS: Conducting experiments, acquiring data, analyzing data, writing the manuscript, approving the final paper.
MG: Conducting experiments, acquiring data, analyzing data, editing the manuscript, approving the final paper
JT: Conducting experiments, acquiring data, analyzing data, editing the manuscript, approving the final paper.
JH: Conducting experiments, acquiring data, analyzing data, approving the final paper.
DW: Conducting experiments, acquiring data, analyzing data, approving the final paper.
BS: Conducting experiments, acquiring data, analyzing data, approving the final paper.
ABR: Conducting experiments, acquiring data, analyzing data, approving the final paper.
JJJ: Conducting experiments, acquiring data, analyzing data, editing the manuscript, approving the final paper.
GK: Conducting experiments, acquiring data, analyzing data, approving the final paper.
JZ: Conducting experiments, acquiring data, analyzing data, approving the final paper.
DL: Conducting experiments, acquiring data, analyzing data, approving the final paper.
SKK: Designing research studies, analyzing data, editing the manuscript, approving the final paper.
JDH: Designing research studies, analyzing data, editing the manuscript, approving the final paper
MMS: Designing research studies, analyzing data, providing reagents, writing the manuscript, editing the manuscript, approving the final paper

Disclosures:

JJJ: Ownership and income, Arvinas, Inc
JT: Yale patent application: New tracers for MMP imaging
DL: Employee of Alexion Pharmaceuticals
SKK: Employee of Alexion Pharmaceuticals
MMS: Spouse employee of Boehringer Ingelheim; Yale patent application: New tracers for MMP imaging

Methods—*Apoe*$^{-/-}$ and *Mmp12*$^{-/-}$/*Apoe*$^{-/-}$ mice were infused with angiotensin (Ang) II. Expression of neutrophil extracellular traps (NETs) markers and complement component 3 (C3) levels were evaluated by immunostaining in aortas of surviving animals. Plasma complement components were analyzed by immunoassay. The effects of a complement inhibitor, IgG-FH$_{1–5}$, and macrophage-specific MMP-12 deficiency on adverse aortic remodeling and death from rupture in AngII-infused mice were determined.

Results—Unexpectedly, death from aortic rupture was significantly higher in *Mmp12*$^{-/-}$/*Apoe*$^{-/-}$ mice. This associated with more neutrophils, citrullinated histone H3 and neutrophil elastase, markers of NETs, and C3 levels in *Mmp12*$^{-/-}$ aortas. These findings were recapitulated in additional models of AAA. MMP-12 deficiency also led to more pronounced elastic laminae degradation and reduced collagen integrity. Higher plasma C5a in *Mmp12*$^{-/-}$ mice pointed to complement overactivation. Treatment with IgG-FH$_{1–5}$ decreased aortic wall NETosis and reduced adverse aortic remodeling and death from rupture in AngII-infused *Mmp12*$^{-/-}$ mice. Finally, macrophage-specific MMP-12 deficiency recapitulated the effects of global MMP-12 deficiency on complement deposition and NETosis, as well as adverse aortic remodeling and death from rupture in AngII-infused mice.

Conclusions—An MMP-12 deficiency/complement activation/NETosis pathway compromises aortic integrity, which predisposes to adverse vascular remodeling and AAA rupture. Considering these new findings, the role of macrophage MMP-12 in vascular homeostasis demands re-evaluation of MMP-12 function in diverse settings.

Graphical Abstract

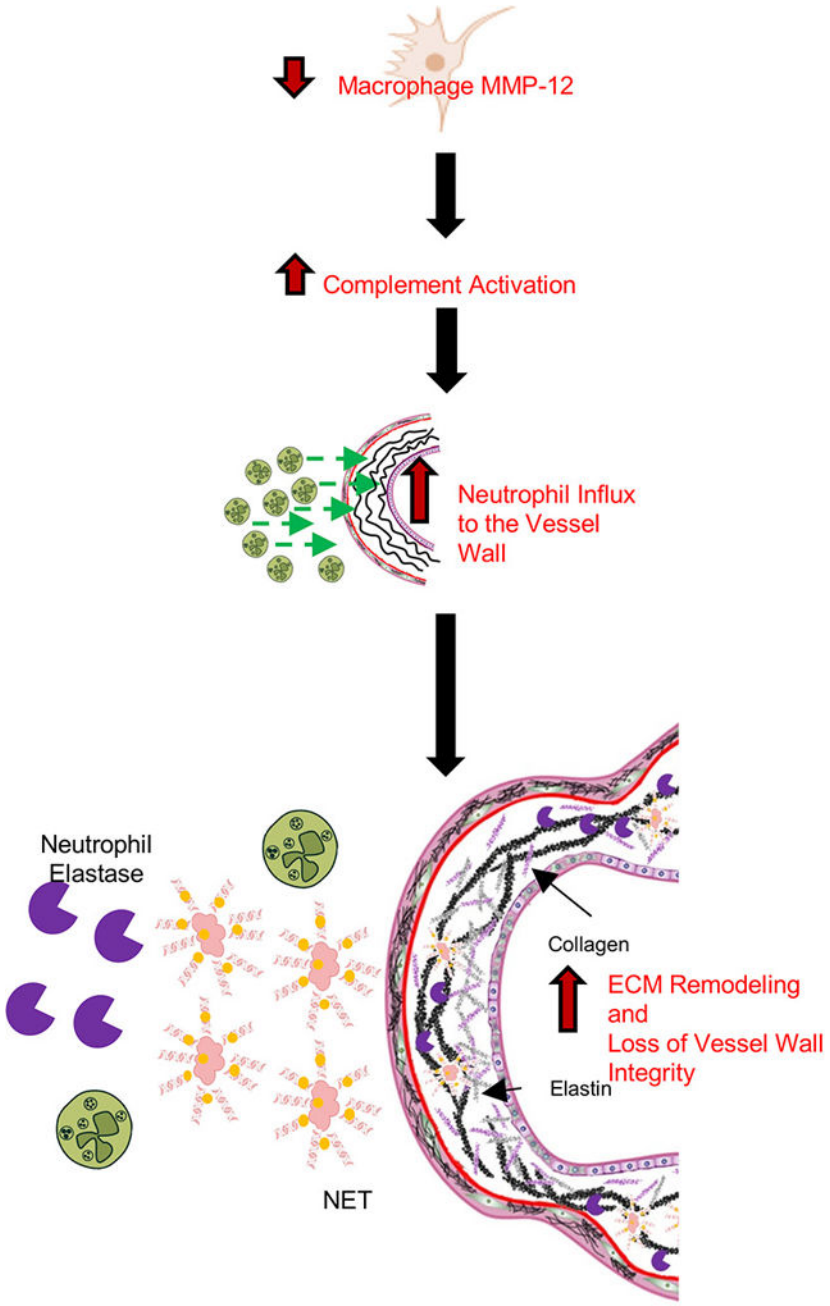

Keywords

Vascular Biology

Introduction

Blood vessels experience pathogens intermittently. Activation of the complement system, a mainstay of immune surveillance, is critical to eliminating these pathogens [1]. If left unchecked, however, complement activation can also perturb the structural integrity and

functionality of the arterial wall, which are normally regulated via homeostatic processes. Control of vascular integrity starts with the endothelial barrier and its interactions with platelets and leukocytes [2, 3]. Extracellular matrix (ECM) and matricellular components of the vascular wall similarly play important roles in maintaining integrity and normal function [4, 5]. Matrix metalloproteases (MMPs) mediate pro-inflammatory signaling, recruitment of inflammatory cells, and degradation of ECM. Accordingly, possible involvement of MMPs in disturbing vascular integrity is often considered in pathologies such as aneurysm, dissection, and rupture [6]. This concept has prompted efforts to develop therapeutics to attenuate MMP activity to prevent adverse vascular remodeling and maintain integrity of the wall [6].

MMP-12 (also known as macrophage elastase) is a protease best known for its elastolytic function. Degradation of elastic fibers is a key component of aneurysm pathogenesis, and MMP-12 is highly upregulated in abdominal aortic aneurysms (AAAs) in humans and multiple mouse models [7, 8]. Nevertheless, a widely held concept regarding the role of MMP-12 in aneurysmal pathogenesis and progression is challenged by studies wherein MMP-12 gene deletion in mice (*Mmp12*$^{-/-}$) has no effect on elastase-induced aneurysm formation [9], despite reducing $CaCl_2$-induced aneurysm development [10] and diminishing aneurysmal rupture in angiotensin (Ang) II-infused mice in the presence of transforming growth factor β neutralization [11]. Emerging data indicate further that, in addition to its elastolytic function, MMP-12 modulates inflammation and immunity through regulation of macrophage and neutrophil function, which depending on the context, can be anti-or pro-inflammatory [12–17]. During our studies aimed at developing specific MMP-12 inhibitors and imaging agents [18], we unexpectedly observed that *Mmp12* deletion promotes rather than prevents AngII-induced AAA development and rupture. Introducing a novel paradigm, we demonstrate that MMP-12 contributes to aortic homeostasis and thus maintaining wall integrity. This finding is linked to the attenuating effect of macrophage MMP-12 on complement overactivation, aortic wall neutrophil infiltration, neutrophil extracellular trap (NET) formation, and elastin degradation.

Methods

Mouse models of AAA.

Apolipoprotein E-null (*Apoe*$^{-/-}$), *Mmp12*$^{-/-}$ (B6.129X-Mmp12^{tm1Sds}/J) and C57BL/6J mice were all purchased from the Jackson Laboratory. *Mmp12*$^{-/-}$/*Apoe*$^{-/-}$ mice were generated in our laboratory by crossing *Apoe*$^{-/-}$ and *Mmp12*$^{-/-}$ mice. B6.129X-Mmp12^{tm1Sds}/J were backcrossed into C57BL/6J by Jackson and 32 SNP panel analysis covering all chromosomes has demonstrated that all markers were C57BL/6. The male sex is a risk factor for AAA development and like humans, male mice are more susceptible to Ang II-induced AAA. Therefore, only male mice were used in the study. For the first model of AAA, 12- to 14-week-old male *Apoe*$^{-/-}$ and *Mmp12*$^{-/-}$/*Apoe*$^{-/-}$ mice were implanted with an osmotic minipump (model 2004 and 2001, Alzet, respectively) delivering recombinant human AngII at 1000 ng/kg/min for up to 4 weeks to induce aneurysm, most often presenting in the suprarenal abdominal aorta (SAA) [19]. To enhance aneurysm formation in *Mmp12*$^{-/-}$ and C57BL/6J mice, 12- to 14-week-old male mice were administered a

single i.p. injection containing 1.0×10^{11} genome copies of recombinant adeno-associated virus (AAV) encoding PCSK9 (AAV8.ApoEHCR-hAAT.D377Y-mPCK9.bGH) obtained from the University of Pennsylvania Vector Core to induce hyperlipidemia accompanied by feeding the mice with a high-fat western diet (HFD) containing 1.25% cholesterol (D12108, Research Diets) [20]. Two weeks later, AAA was induced by following the above procedure. For the second model of AAA, 12- to 14-week-old male *Apoe*$^{-/-}$ and *Mmp12*$^{-/-}$/*Apoe*$^{-/-}$ mice were used to generate infrarenal abdominal aortic aneurysm as described previously [21]. Briefly, animals were treated with β-aminopropionitrile (BAPN, Sigma) 0.2 % in drinking water. Two days after the start of BAPN administration, the animals underwent surgery. The infrarenal abdominal aorta was exposed, and porcine pancreatic elastase (6.67 mg/mL, 10 U/mg, MP Biomedical) was applied topically for 5 min. At 4-weeks after surgery, the surviving animals were euthanized for tissue collection.

Generation of *Mmp12*$^{-/-}$/*Apoe*$^{-/-}$ and conditional macrophage-specific *Mmp12*$^{-/-}$ mice.

To generate *Mmp12*$^{-/-}$/*Apoe*$^{-/-}$ mice, B6.129X-Mmp12^{tm1Sds}/J mice from Jackson Laboratory (Stock No: 004855) [22] were crossed with B6.129P2-*Apoe*^{tm1Unc}/J mice (ApoE KO, Jackson Lab, Stock No: 002052). Genome scanning of *Mmp12*$^{-/-}$/*Apoe*$^{-/-}$ mice by Jackson laboratories showed 95% of the single nucleotide polymorphism panel was of C57BL/6J background. To generate macrophage-specific *Mmp12* deficient mice, C57BL/6N *Mmp12*$^{tm1a(EUCOMM)Hmgu/H}$ mice from Infrafrontier GmbH (Munich, Germany, European Mouse Mutant Archive ID:05321) that contain FRT and loxP sites were then crossed with B6.Cg-Tg(Pgk1-flpo)10Sykr/J (FLPo-10, Jackson Lab, Stock No: 011065) to generate *Mmp12*$^{flox/flox}$ Mice. Next, the FVB macrophage-specific (Csf1r promoter), tamoxifen-inducible Cre-expressing Tg(Csf1r-Mer-iCre-Mer)1Jwp transgenic mice from Jackson Laboratory (Stock No: 019098) [23] were crossed with *Mmp12*$^{flox/flox}$ mice. *Mmp12* deletion in macrophages was induced by daily intraperitoneal injection of tamoxifen (Sigma-Aldrich, T5648–1G, dissolved in corn oil) at 75 mg/kg of mouse body weight, every 24 hours for a total of 5 consecutive days with a 7-day waiting period after the final injection for recombination.

Blood pressure measurements.

Arterial blood pressure was measured continuously in a sub-group of *Apoe*$^{-/-}$ and *Mmp12*$^{-/-}$/*Apoe*$^{-/-}$ mice using radiotelemetry for 3 days prior to and up to 9 days after the implantation of AngII-infusing minipump. The blood pressure transducer (TA11PA-C10; Data Sciences International) [24] was introduced via a catheter implanted in the left common carotid artery.

Tissue processing, histology, morphometry, and immunostaining.

Animals euthanized at the desired time point were perfused with heparinized saline solution. The aorta was carefully harvested and used for aortic cell isolation and flow cytometry experiments or placed in Optimal Cutting Temperature compound (Tissue Tek), snap frozen, and processed using a cryostat (CM1850, Leica). Serial sections were collected at regular intervals and used for morphometry and immunofluorescence staining.

For morphometric analysis, serial tissue sections of the abdominal aorta were collected and imaged using a microscope (Eclipse E400, Nikon). For tissues with aneurysm, the maximal external diameter was selected for staining and measured using ImageJ/Fiji software (https://imagej.nih.gov/ij/). For immunofluorescence staining, sections were fixed with 4% paraformaldehyde in PBS for 20 min at room temperature followed by blocking with either 10% normal goat serum or 2% bovine serum albumin in PBS for 1 hour. The tissue sections were then incubated overnight at 4 °C with primary antibodies: anti-Ly6G clone 1A8: 1:100, BP0075–1, Bio X Cell; anti-Histone H3 (citrulline R2 + R8 + R17): 1:100, ab5103, Abcam; anti-neutrophil elastase: 1:100, ab68672, Abcam; anti-mouse complement component 3 (C3), 55463, MP Biomedicals; anti-tropoelastin antibody: 1:100, ab21600, Abcam; anti-C3d biotinylated: 1:200, BAF2655, R&D Systems; anti-CD68, 1:100, ab53444, Abcam; anti-CD31/PECAM-1, 1:100, MAB1398Z, Millipore Sigma; anti-α-smooth muscle actin, 1:100, A2547,Sigma-Aldrich. Isotype-matched immunoglobulin preparations were used as control to establish staining specificity. The sections were then incubated for 1 hour in a 1:200 dilution of appropriate Alexa Fluor 555 (A-48270, S32355, Thermo Fisher Scientific) or 594-conjugated secondary antibodies (S32356, A-11007 or A-11012, Thermo Fisher Scientific) followed by 4′,6-diamidino-2-phenylindole (DAPI) staining (Thermo Fisher Scientific). Mouse *Mmp12* RNA transcripts were detected by fluorescence in situ hybridization (HuluFish Plus kit, Atto647-MMP-12, Q2022016) following the manufacturer's protocol. After washing, the slides were mounted using Prolong Diamond Antifade Mountant (Thermo Fisher Scientific). The images were acquired using a fluorescence microscope (DMi8, Leica) and quantified using ImageJ software. Verhoeff-Van Gieson (VVG) staining was performed on tissue sections according to standard protocols by Yale Pathology Tissue Services. Collagen Hybridizing Peptide, Cy3 Conjugate (R-CHP, 3Helix) was used to stain for single stranded collagens. Briefly, a solution of the peptide with a concentration of 20 μM was heated to 80°C for 5 min in a water bath in a sealed microtube followed by quenching in an ice-water bath for 15–90 s and subsequently applied to the tissues and incubated overnight at 4 °C. Finally, images which best represented the overall results were selected and presented as figures.

Quantitation of C3 and complement component 5a (C5a) in mouse plasma.

Mouse plasma C3 or C5a was quantified using a Gyrolab xPlore automated immunoassay system (Gyros Protein Technologies). For plasma C3 assay, the biotin-labeled complement C3-specific monoclonal capture antibody (11H9, Novus NB200–540B) was formulated at 100 μg/mL and Alexa Fluor 647-labeled anti-C3 antibody (MP Biomedicals, 55463) was formulated at the working concentration of 5 μg/mL in Rexxip F buffer (Gyros Protein Technologies, P0004825) for detection of C3. The standard curve for C3 was prepared using purified mouse C3 (CompTech, M113) which was serially diluted and spiked into Rexxip A buffer. The capture and detection antibodies, standards and unknown plasma samples were placed in the predetermined locations in a PCR plate (Gyros Protein Technologies, P0004861) per manufacturer's recommendation. Biotin-labeled anti-C3 capture antibody was immobilized on the surface of streptavidin-coated Gyrolab Bioaffy CD200 (Gyros Protein Technologies, P0004180) and plasma samples were loaded. Captured C3 was detected by Alexa Fluor 647-labeled anti-C3 antibody. For C5a quantification, the biotin-labeled monoclonal capture antibody (R&D, MAB21501) was formulated at 100 μg/m and

Alexa Fluor 647-labeled anti-C5a antibody (R&D, AF2150) was formulated at 5 μg/mL in Rexxip F buffer (Gyros Protein Technologies, P0004825). The standard curve was prepared by spiking recombinant mouse C5a (R&D, 2150-C5–025) at 150 ng/mL and serially diluting 3-fold in C5-deficient NOD-SCID mouse plasma (BIOIVT, MSE61PLKZYNN). The immune assay then run as described in C3 assay. Concentrations of samples were calculated using Gyrolab software.

Quantitative Reverse transcription polymerase chain reaction (RT-PCR).

Total RNA was isolated from normal aorta (suprarenal abdominal aorta) as well as bone marrow-derived macrophages (RNeasy Mini Kit, Qiagen) and reverse transcribed (QuantiTect Reverse Transcription Kit, Qiagen). RT-PCR was performed on a Real-Time PCR System 7500 (Applied Biosystems) using the following TaqMan primers and probe sets (β-actin: Mn00607939_s1, Elastin: Mm00514670_m1, *Eln*: Mm00500554_m1, *Mmp12*, Thermo Fisher Scientific). Reactions were run in triplicates on the 7500 real-time PCR system (Thermo Fisher Scientific) and experimental gene expression was normalized to that of β-actin.

Flow cytometry.

Carefully harvested whole aortas were cut in < 1 mm pieces and incubated in a mixture of enzymes (400 U/ml collagenase type I, 120 U/ml collagenase type XI, 60 U/ml hyaluronidase, 60 U/ml DNase1 in PBS-HEPES 20 mM) at 37°C for 1 hour. The tissue was filtered using a 70 μm cell strainer and aortic cells were resuspended in PBS-FBS 2%. After Fc receptor blocking (Mouse BD Fc Block, BD Biosciences) for 20 min at room temperature, cells were labeled with PE-conjugated anti-mouse CD45 (BioLegned, Cat. No. 103105), APC-conjugated anti-mouse Ly6G (BD Biosciences, Cat. No. 560599) and Alexa Fluor 488-conjugated anti-mouse CD11b (BD Biosciences, Cat. No. 557672) antibodies for 20 min on ice, and used for flow cytometry (LSR II, BD Bioscience) with 7-AAD (Thermo Fisher Scientific, Cat. No. A1310) to verify cell viability. Data were processed using FlowJo Software. Forward and side scatter density plots were used to exclude debris and to identify single cells. Following selection of 7-AAD- live cells and gating on CD45+ cells, the CD11b and Ly6G signals were further analyzed to identify macrophage and neutrophil populations. An outline of the gating strategy is shown in Fig. S1.

Isolation of Bone Marrow-derived macrophages.

Mmp12$^{-/-}$ bone marrow-derived macrophages (BMDMs) derived from Csf1r-Mer-iCre-Mer:*Mmp12*$^{flox/flox}$ mice were isolated using a previously established method [25]. Briefly, bone marrow cells were harvested and cultured in Dulbecco's Modified Eagle Medium/F12 (DMEM/F12; Thermo Fisher Scientific, Cat. No. 11320033) supplemented with 10% (v/v) fetal bovine serum (FBS; Hyclone), 100 IU/ml penicillin, 100 μg/ml streptomycin (DMEM/F12–10) and 10 ng/mL macrophage colony–stimulating factor (M-CSF; Enzo Life Sciences, ENZ-PRT144–0010). The harvested cells were counted in a hemacytometer and adjusted to a concentration of ~4×10^6 /ml in the medium. Then, a total of 4×10^5 cells were added to each sterile plastic petri dish in 10 mL medium and incubated in an incubator at 37°C, and 5% CO_2. On day 3, another 5 ml of macrophage complete medium was added to each dish.

After 7 days in culture, nonadherent cells are discarded and adherent cells were harvested for RNA isolation.

Anti-complement treatment protocol.

12–18-week-old mice were injected intraperitoneally with a fusion protein consisting of factor H regulatory domains linked to a non-targeting mouse immunoglobulin (IgG-$FH_{1–5}$, 56 mg/kg), anti-C5 antibody (BB5.1, 40 mg/kg) or control IgG_1 MOPC (40 mg/kg), provided by Alexion Pharmaceuticals (New Haven, CT), every 3 days for 9 days prior to AAA induction and the treatment with IgG-$FH_{1–5}$ or MOPC continued for up to 28 days until completion of the study.

Burst pressure tests.

The descending thoracic aorta (from the first to fifth pair of intercostal arteries) and the suprarenal abdominal aorta (from the diaphragm to right renal artery) were excised and cleaned of perivascular tissue, then their branches were ligated to allow ex vivo pressurization. The vessels were cannulated and ligated on glass pipettes and placed within a custom computer-controlled extension-inflation mechanical testing device [26]. Following both a 15-min acclimation of the specimen within a Hank's buffered salt solution (HBSS) at room temperature (to negate smooth muscle contractility, thus focusing on ECM strength) and 90 mmHg pressure and four preconditioning cycles consisting of pressurization from 10 to 140 mmHg at a fixed value of axial stretch, the in vivo value of axial stretch was estimated for each sample as the value at which the transducer-measured axial force does not change appreciably during cyclic pressurization [27]. Once done, the samples were re-cannulated on a custom blunt-ended double-needle assembly, stretched to the estimated in vivo axial length, and pressurized to failure, as described previously [28].

Statistics.

All values are expressed as median and interquartile range (Q_1-Q_3). Data were compared using two-tailed Mann-Whitney U test, Kruskal-Wallis with Dunn's multiple comparisons post hoc test as appropriate. Kaplan-Meier survival curves were compared using Log-rank (Mantel-Cox) test. We did not apply any experiment-wide or across-test multiple testing correction and a P value < 0.05 was considered significant. No animal was excluded over the course of this study. Randomization and blinding were not applied as these measures were not applicable for the comparisons carried out throughout the study.

Study approval.

All animal procedures were performed in accordance with protocols approved by Yale University and Veterans Affairs Connecticut Healthcare System Institutional Animal Care and Use Committees.

Results

MMP-12 deficiency promotes AAA development and rupture

To examine the role of MMP-12 in AAA, *Apoe*$^{-/-}$ and *Mmp12*$^{-/-}$/*Apoe*$^{-/-}$ mice were infused with AngII at 1000 ng/kg/min. Consistent with previous reports [19, 29, 30], this led to death due to aortic rupture in a subset of *Apoe*$^{-/-}$ mice by 4 weeks after initiating the AngII infusion. Unexpectedly, death from rupture was significantly greater in *Mmp12*$^{-/-}$/*Apoe*$^{-/-}$ mice, with a cumulative probability of survival to 7 days of only 14% for *Mmp12*$^{-/-}$/*Apoe*$^{-/-}$ compared to 71% for *Apoe*$^{-/-}$ mice (Fig.1A). To investigate whether a change in blood pressure response to AngII infusion influenced this difference in survival, systolic and diastolic blood pressures were measured in *Apoe*$^{-/-}$ and *Mmp12*$^{-/-}$/*Apoe*$^{-/-}$ before and after AngII initiation. As shown in Fig. S2, there was no significant difference in either blood pressure or heart rate between the two groups of animals. In addition, evaluation of total cholesterol levels showed no difference between the two group of animals (Fig. S3).

As inflammatory cell recruitment can play a key role in early stages of aneurysm development [31], we evaluated the effect of *Mmp12* deletion on aortic macrophage and neutrophil concentrations before and after AngII infusion. Due to early loss of AngII-infused *Mmp12*$^{-/-}$/*Apoe*$^{-/-}$ mice, cell infiltration was measured at 18–24 h post AngII infusion. Flow cytometry revealed a significant increase in CD45^{+} cells in both *Apoe*$^{-/-}$ and *Mmp12*$^{-/-}$/*Apoe*$^{-/-}$ mice (Fig. 1B). Evaluation of the percentage of CD11b^{+}/Ly6G^{-} mononuclear myeloid cells, primarily macrophages, among live cells showed no significant difference at this time post-AngII infusion compared to baseline in either *Apoe*$^{-/-}$ or *Mmp12*$^{-/-}$/*Apoe*$^{-/-}$ mice and no difference between the two groups of animals (Fig. 1C). Importantly, however, AngII infusion significantly increased aortic CD11b^{+}/Ly6G^{+} neutrophils in both *Apoe*$^{-/-}$ and *Mmp12*$^{-/-}$/*Apoe*$^{-/-}$ mice with a significantly higher percentage of neutrophils detected post-AngII infusion in *Mmp12*$^{-/-}$/*Apoe*$^{-/-}$ mice compared to *Apoe*$^{-/-}$ animals, suggesting that MMP-12 may regulate neutrophil recruitment to the vessel wall (Fig. 1D).

This significant difference in aortic wall neutrophil infiltration was also detected by Ly6G immunostaining in animals surviving to day 7 post-AngII infusion, with significantly higher neutrophil staining in remodeled SAA in *Mmp12*$^{-/-}$/*Apoe*$^{-/-}$ mice compared to *Apoe*$^{-/-}$ animals (Fig 1E). This led us to assess the effect of *Mmp12* deletion on aortic wall NETosis. Immunostaining for citrullinated histone H3 (Cit-H3) and neutrophil elastase (NE), as markers of NET, was also significantly greater in *Mmp12*$^{-/-}$/*Apoe*$^{-/-}$ mice compared to *Apoe*$^{-/-}$ animals (Fig 1E). Strikingly, while neutrophil, Cit-H3, and NE levels were barely detectable in the SAA of *Apoe*$^{-/-}$mice at baseline without AngII infusion, significantly higher neutrophil, Cit-H3, and NE levels were present in the SAA of *Mmp12*$^{-/-}$/*Apoe*$^{-/-}$ mice even at baseline (Fig. 1F).

The effect of MMP-12 deficiency on aneurysm development was confirmed in a second murine model, where infrarenal AAA is induced by a combination of oral β-aminopropionitrile (BAPN) administration and peri-vascular elastase application in *Apoe*$^{-/-}$ mice. While no significant difference was observed in animal survival to 28 days between *Apoe*$^{-/-}$ and *Mmp12*$^{-/-}$/*Apoe*$^{-/-}$ mice (Fig. S4A), the maximal external diameter of

infrarenal abdominal aorta (IAA) was significantly larger in *Mmp12*$^{-/-}$/*Apoe*$^{-/-}$ mice [2.90 (2.44–3.19) mm] than in *Apoe*$^{-/-}$ mice [1.50 (1.17–2.25) mm, $P < 0.01$, Fig. S4B and C] that survived 28 days following surgery. In line with the observations in the first model of AAA, MMP-12 deficiency associated with significantly higher IAA Ly6G-positive neutrophil infiltration and NET deposition in these animals, as evidenced by Cit-H3 and NE immunostaining (Fig. S4D).

Unlike its effect in *Apoe*$^{-/-}$ mice, AngII infusion has a modest effect on AAA induction and animal survival in normolipidemic wild-type (WT) C57BL/6 mice [19]. Therefore, to examine whether the effect of *Mmp12* deletion on aneurysm development extends to WT animals, we induced hyperlipidemia in *Mmp12*$^{-/-}$ and WT mice using a combination of adenovirus expressing gain-of-function proprotein convertase subtilisin/kexin type 9 (AAV8-PCSK9) and a HFD [32]. Measurement of total blood cholesterol demonstrated increases in both WT and *Mmp12*$^{-/-}$ mice upon AAV8-PCSK9/HFD administration, and no significant differences between these two groups before or after this intervention (Fig. S5). AngII infusion in these hyperlipidemic animals resulted in significantly lower survival probability at 4 weeks for *Mmp12*$^{-/-}$ (45%) than WT (77%) mice (Fig. 2A). Furthermore, the maximal external diameter of SAA in hyperlipidemic *Mmp12*$^{-/-}$ mice that survived to 28 days of AngII infusion [1.79 (1.46–2.84) mm] was significantly larger than the corresponding aortic diameter in hyperlipidemic WT animals [0.93 (0.85–0.99) mm, *P<0.01*, Fig. 2B]. This difference associated with higher SAA neutrophil and NET levels, as detected by immunostaining, in these *Mmp12*$^{-/-}$ mice compared to WT animals (Fig. 2C). Like *Mmp12*$^{-/-}$/*Apoe*$^{-/-}$ mice, significantly higher neutrophil infiltration and NET deposition was detectable at baseline, without AngII infusion, in hyperlipidemic *Mmp12*$^{-/-}$ mice compared to hyperlipidemic WT animals (Fig. 2D).

Aortic wall integrity is compromised in the absence of MMP-12

ECM proteins play key roles in maintaining aortic wall integrity, with mechanical properties of the aorta determined largely by elastic fibers and fibrillar collagen [33]. VVG staining revealed disrupted elastic laminae with dense and irregular fibers in *Mmp12*$^{-/-}$/*Apoe*$^{-/-}$ and *Mmp12*$^{-/-}$ mice (Fig. 3A). This was associated with significantly higher tropoelastin expression in these animals, as detected by immunostaining (Fig. 3B and C) and RT-PCR (Fig. S6), than in *Apoe*$^{-/-}$ and WT mice. MMP-12 deficiency also associated with increased collagen remodeling, with higher collagen I (Fig. 3D and E) and single stranded collagen α-chains (Fig. 3F and G) detected by immunostaining in *Mmp12*$^{-/-}$/*Apoe*$^{-/-}$ and *Mmp12*$^{-/-}$ mice than in *Apoe*$^{-/-}$ and WT mice. Together, these results point to extensive aortic wall ECM remodeling in the absence of MMP-12, though without insight into the structural competence of the synthesized fibers. Comparison of the burst pressure, an indicator of the biomechanical strength of the aorta, showed significantly lower values in both the descending thoracic aorta and suprarenal abdominal aorta of *Mmp12*$^{-/-}$/*Apoe*$^{-/-}$ mice compared to *Apoe*$^{-/-}$ animals [respectively, 516 (425–597) vs 729 (651–989) mmHg, $P < 0.05$, and 422 (334–474) vs 553 (476–749) mmHg, $P < 0.05$, Fig. 3H].

Complement overactivation mediates the effect of MMP-12 deficiency on aortic wall NETosis

Aortic wall neutrophil infiltration and NETosis in the absence of MMP-12, in conjunction with the interplay between complement overactivation and NETosis, [34] led us to investigate roles of the complement system in the aforementioned observations. Immunofluorescence staining showed significantly higher C3 deposition in *Mmp12*$^{-/-}$/*Apoe*$^{-/-}$ and *Mmp12*$^{-/-}$ aortas compared to *Apoe*$^{-/-}$ and WT vessels, respectively, potentially pointing to aberrant complement activation in MMP-12-deficient mice (Fig. 4A and B). Analysis of plasma complement components showed significantly lower C3 levels in both *Mmp12*$^{-/-}$/*Apoe*$^{-/-}$ vs *Apoe*$^{-/-}$ [313 (253–371) vs 1600 (1473–1912) μg/ml, P <0.01] and *Mmp12*$^{-/-}$ vs WT [528 (465–800) vs 1565 (1182–1979) μg/ml, P < 0.05] mice, indicating a dysregulation of complement system with higher C3 consumption. This was associated with higher levels of C5a, a potent chemoattractant anaphylatoxin for neutrophils, in *Mmp12*$^{-/-}$/*Apoe*$^{-/-}$ vs *Apoe*$^{-/-}$ [79 (66–94) vs 56 (45–70) ng/mL, P < 0.05] and *Mmp12*$^{-/-}$ vs. WT [88 (56–119) vs 48 (44–52) ng/mL, P < 0.05] mice (Fig. 4C and D).

Next, we assessed the efficacy of different strategies in blocking complement activation and potentially clearing NET deposits in MMP-12 deficient animals. Administration of an anti-C5 antibody (BB5.1), which inhibits C5 activation, for 9 days at doses typically used for in vivo blocking studies [35] did not have any significant effect on C3 plasma levels but modestly reduced NET deposits in the vessel wall in *Mmp12*$^{-/-}$ mice (Fig. S7). Therefore, we assessed the efficacy of an upstream inhibitor of complement alterative pathway (AP) activation, IgG-FH_{1-5}, a fusion protein consisting of factor H regulatory domains (FH_{1-5}) linked to a non-targeting mouse immunoglobulin [36]. Plasma analysis confirmed the consistent presence of FH_{1-5} in *Mmp12*$^{-/-}$/*Apoe*$^{-/-}$ mice injected with the inhibitor (56 mg/kg, i.p.) every three days (Fig. S8). Inhibition of AP activity by IgG-FH_{1-5} treatment resulted in significantly increased plasma C3 levels in *Mmp12*$^{-/-}$/*Apoe*$^{-/-}$ [603 (529.5–776) μg/mL at Day 0 vs 1100 (824–1440) μg/mL at Day 9, P < 0.01] and *Mmp12*$^{-/-}$ [637 (507–957) μg/mL at Day 0 vs 1305 (1110–1486) μg/mL at Day 9, P < 0.05] mice (Fig. 4E and F). The increase in plasma C3 level associated with a significant decrease in aortic C3 deposition in MMP-12 deficient mice (Fig. 4G and H). More importantly, IgG-FH_{1-5} treatment markedly cleared the aortic wall NETosis, as detected by Cit-H3 immunostaining, in both *Mmp12*$^{-/-}$/*Apoe*$^{-/-}$ and *Mmp12*$^{-/-}$ mice (Fig. 4I and J).

Complement inhibition ameliorates aneurysm development and rupture in *Mmp12*$^{-/-}$ mice

Given the effect of complement inhibition in clearing NET deposits in MMP-12 deficient mice, and the role of NETosis in aneurysm development [37], we sought to determine whether IgG-FH_{1-5} can reverse the effect of MMP-12 deficiency on AAA development and rupture. MMP-12-deficient mice pre-treated with IgG-FH_{1-5} for 9 days were infused with AngII for 28 days while the treatment continued. Compared to the control IgG_1 (MOPC-31C) antibody, IgG-FH_{1-5} treatment had no significant effect on survival in the more aggressive phenotype, *Mmp12*$^{-/-}$/*Apoe*$^{-/-}$ mice (Fig. S9). However, in the less severe, *Mmp12*$^{-/-}$-AAV8-PCSK9/HFD model, IgG-FH_{1-5}-treatment significantly improved survival probability compared to control IgG_1 (80% vs 40%, P < 0.05, Fig. 5A). Furthermore, the maximal SAA external diameter in IgG-FH_{1-5}-treated mice that survived to 28 days

[1.20 (0.96–1.60) mm] was significantly lower than the corresponding aortic diameter in *Mmp12*$^{-/-}$ animals treated with control IgG_1 [2.04 (1.61–2.50] mm, $P < 0.05$, Fig. 5B). Moreover, in surviving IgG-$FH_{1–5}$-treated mice, aortic wall C3d deposition was significantly lower compared to the control group (Fig. 5C), and IgG-$FH_{1–5}$ significantly decreased neutrophil infiltration and NET deposits in the remodeled aortic wall of AngII-infused *Mmp12*$^{-/-}$ mice compared to the control antibody (Fig. 5D).

Macrophage MMP-12 deficiency recapitulates the effect of global MMP-12 deficiency on aortic wall complement deposition and NETosis

Macrophages are a major source of MMP-12. Therefore, to determine whether the MMP-12 involved in regulating vascular integrity originates in macrophages, *Mmp12*$^{flox/flox}$*/Csf1r-iCre* and *Mmp12*$^{flox/flox}$*/Apoe*$^{-/-}$*/Csf1r-iCre* mice were generated. Inducible ablation of *Mmp12* was confirmed in cultured bone marrow-derived macrophages (BMDMs) from *Mmp12*$^{flox/flox}$*/Apoe*$^{-/-}$*/Csf1r-iCre* and *Mmp12*$^{flox/flox}$*/Csf1r-iCre* mice treated with tamoxifen for 5 consecutive days (Fig. 6A and 6B). *Mmp12* fluorescence in situ hybridization in conjunction with immunostaining of aortic sections from tamoxifen-treated mice confirmed *Mmp12* deletion in macrophages with no detectable effect in endothelial cells or vascular smooth muscle cells (Fig. S10 and S11). This was associated with significantly higher neutrophil, NET, NE and C3d staining in tamoxifen treated *Mmp12*$^{flox/flox}$*/Apoe*$^{-/-}$*/Csf1r-iCre* and *Mmp12*$^{flox/flox}$*/Csf1r-iCre* mice compared to control, *Mmp12*$^{flox/flox}$*/Apoe*$^{-/-}$ and *Mmp12*$^{flox/flox}$ mice (Fig. 6C and 6D). Furthermore, higher collagen and tropoelastin levels were observed in both *Mmp12*$^{flox/flox}$*Csf1r-iCre* and *Mmp12*$^{flox/flox}$*/Apoe*$^{-/-}$*/Csf1r-iCre* mice compared to control (Fig. S11). AngII infusion resulted in significantly lower 7-day survival in *Mmp12*$^{flox/flox}$*/Apoe*$^{-/-}$*/Csf1r-iCre* compared to *Mmp12*$^{flox/flox}$*/Apoe*$^{-/-}$ (Fig. 6E). In addition, the maximal SAA external diameter of surviving mice was significantly higher in *Mmp12*$^{flox/flox}$*/Apoe*$^{-/-}$*/Csf1r-iCre* [1.99 (1.20–2.54) mm] compared to *Mmp12*$^{flox/flox}$*/Apoe*$^{-/-}$ mice [0.90 (0.83–0.98) mm, $P < 0.01$, Fig. 6F].

Discussion

This study provides new insight into MMP-12 as a key contributor to aortic homeostasis. In the absence of MMP-12, activation of the complement system leads to NETosis and adverse ECM remodeling, including degradation of elastic laminae and compromised collagen integrity. Combined, these changes reduce aortic wall strength and can predispose the aorta to dilatation and rupture in the presence of aneurysmal stimuli.

Elevated MMP-12 expression in human AAA specimens, in conjunction with elastase activity and association with residual elastic fiber fragments, contributed to the prevailing paradigm that MMP-12 has a direct role in promoting AAA pathogenesis, progression, and rupture [7]. This presumed role of MMP-12 in the natural history of AAA is challenged, however, by a finding in *Mmp12*$^{-/-}$ mice that MMP-12 deficiency has no effect on elastase-induced aneurysm formation [9], despite its deficiency reducing $CaCl_2$-induced aneurysm development [10] and diminishing aneurysm rupture in AngII-infused mice in the presence of transforming growth factor β neutralization [11]. Our data show that macrophage MMP-12

contributes to the maintenance of aortic integrity and its deficiency promotes aneurysm development and rupture triggered by Ang II or elastase/BAPN in three murine models of AAA in the presence or absence of apolipoprotein E deficiency. Although differences across these studies depend, in part, on the specific mouse model studied, including differences in genetic background (129 in [9] and [10] vs C57BL6 in [11] and the present study) [38], the experimental trigger for aneurysm (elastase [9] vs $CaCl_2$ [10] or Ang II [11]), and the biological context (transforming growth factor β neutralization [11] vs absence of apo E vs no such intervention), our data support a challenge to the prevailing paradigm. A similar discrepancy exists regarding MMP-2 and MMP-9 deficiency. Ang II infusion (1500 μg/kg/day) leads to more severe aortic dilatation in *Mmp2*$^{-/-}$ mice compared to WT controls [39] and MMP-9 deficiency promotes Ang II (1 μg/kg/min)-induced aortic rupture in *Apoe*$^{-/-}$ mice [40]. Conversely, MMP-2 and MMP-9 deficiency protects mice from $CaCl_2$-induced aortic aneurysm [39, 41]. Notably, collagenase resistance in *Col*$^{R/R}$/*Apoe*$^{-/-}$ mice, which leads to accumulation of fibrillar collagen promotes the disruption of elastic laminae and accelerates Ang II-induced AAA development [42]. Similarly, we show that the effect of MMP-12 deficiency on aortic integrity extends beyond the response to Ang II infusion, and there are major biological and structural changes in the aorta in the absence of any other manipulation.

The detrimental effect of MMP-12 deficiency [which was not associated with any significant difference in aortic *Mmp2*, *Mmp3*, *Mmp9* and *Mmp13*, or *Timp2* and *Timp3* mRNA expression between *Apoe*$^{-/-}$ and *Mmp12*$^{-/-}$/*Apoe*$^{-/-}$ mice (not shown)] does not necessarily indicate that higher levels of MMP-12 is beneficial in AAA. MMPs are multifunctional proteases, and their proteolytic actions can result in the release of additional biologically active molecules. In the absence of MMP-12, there is neutrophil infiltration and high levels of neutrophil elastase in the vessel wall, which may contribute to elastin degradation and vessel wall weakening. In this regard, some studies have reported biphasic actions of MMPs, for instance, in the context of stroke, where MMPs initially have a deleterious effect but subsequently aid in remodeling and recovery [43]. Considering the multifaceted functions of MMPs, it would not be surprising if MMP-12 is found to have different effects at different levels and in different stages of aneurysm development.

While *Mmp12*$^{-/-}$ mice have been studied for more than two decades, they are not known to exhibit overt cardiovascular abnormalities. Our finding that MMP-12 deficiency has profound effects on vessel wall structural integrity raises the possibility that missing this baseline abnormality may have affected the interpretation of some, if not most of the previous studies in this area. Indeed, while many of the earlier studies focused on the role of MMP-12 as an elastase, more recent studies indicate that MMP-12 also plays protective roles by resolving inflammation in rheumatoid arthritis [44, 45], attenuating lipopolysaccharide-induced lung inflammation [12], limiting myocardial infarction [16], and defending against bacterial [13] and viral [14] infections. In this context, our findings introduce a new paradigm regarding the role of MMP-12 in vascular biology that may have major implications regarding the role of this metalloproteinase in other pathologies.

The complement system consists of a complex array of proteins arranged in a proteolytic cascade that, once activated, produces potent effector molecules impacting innate and

adaptive immunity. The three complement pathways that initiate the cascade (classical, lectin, and alternative) all culminate in the generation of C3 convertases, which cleave C3 into C3a (a chemotactic mediator of inflammation) and C3b (an opsonin), and subsequently C5 convertases cleaving C5 into C5a (another chemotactic mediator of inflammation) and C5b, which mediates the assembly of membrane attack complex [46, 47]. A low-level constitutive activation of the alternative pathway (AP), the so-called tick-over phenomenon, is an integral part of immune surveillance to monitor the presence of pathogens [46]. Activation and amplification of the AP is tightly regulated by soluble and membrane-associated regulators. Several studies have demonstrated the presence of activated complement components in human and experimental vascular pathologies, including AAA [48], and blocking the activity of properdin, a positive regulator of AP, has prevented elastase-induced murine AAA [49]. Similarly, we observed considerable complement activation, as manifested by aortic wall C3 deposits and a reduction in plasma C3 levels in our murine models of AAA, and IgG-$FH_{1–5}$ treatment reduced vascular remodeling and aneurysm rupture.

Complement activation in the absence of MMP-12 and its inhibition by IgG-$FH_{1–5}$ in our study point to the activation of the AP and suggests that MMP-12 serves as a negative regulator of complement activation. This is in line with a recent proteomic analysis of MMP-12 substrates that identified several members of the complement system, including C3, C3a and C5a, as MMP-12 substrates [44]. The functional significance of this MMP-12 effect has been shown in a model of collagen-induced arthritis, where higher levels of inflammation and tissue damage occurred in *Mmp12*$^{-/-}$ mice (on a 129Sv/Ev background). Interestingly, no difference was observed at baseline between these animals and wild-type controls. This is in contrast with our observation in *Mmp12*$^{-/-}$ mice (on a C57BL/6J background), which exhibited considerable systemic complement activation and complement deposition that could be resolved with administration of IgG-$FH_{1–5}$, suggesting that MMP-12 deficiency may potentiate the low-level tick-over complement activation and render the aorta more prone to adverse effects. As such, MMP-12 is a key component of homeostatic mechanisms that maintain vessel wall integrity. There is, however, a need to consider further the possible role of modifier genes given the different results in mice having different backgrounds.

Complement activation can trigger NET formation and NETs can serve as a platform for complement activation [34]. NETs, extracellular meshes of chromatin and granule proteins, are released by neutrophils primarily through a cell death process, NETosis [50]. This process and non-lytic NET release are major players in the immune defense against pathogens. If left unchecked, however, this process can lead to excessive tissue damage by promoting complement activation, inflammation, and thrombosis. Several vascular pathologies, including atherosclerosis and AAA, associate with NETosis. Indeed, NETs contain large quantities of neutrophil elastase, a key protease in AAA formation [51] and treatment with the NETosis inhibitor, Cl-amidine, attenuates adverse vascular remodeling in AAA [52]. Similarly, our study associated AAA formation with complement activation and NETosis in three distinct murine models. Moreover, these processes were amplified in the absence of MMP-12, which exacerbated vascular remodeling and aneurysm rupture in *Mmp12*$^{-/-}$ mice. Importantly, MMP-12 deficiency also led to vessel wall neutrophil

infiltration and NETosis in the absence of AAA induction, which cleared upon IgG-$FH_{1–5}$ treatment. This NETosis associated with elastic laminae degradation and frustrated collagen remodeling, which manifested functionally as a weakened aortic wall with lower burst pressure. Burst pressure studies of aortas from MMP-12 deficient mice revealed lower values in both the descending thoracic and suprarenal abdominal aorta. Regardless of the presence or absence of MMP-12, and as reported by others [39, 53, 54], Ang II infusion led to the development of aneurysm (and dissection) in the suprarenal abdominal aorta and occasionally, thoracic aorta. Combined, these data link MMP-12 deficiency to complement activation and NETosis of the aorta, which promotes vessel wall inflammation, weakens the vessel wall, and predisposes the aorta to adverse remodeling and rupture in response to aneurysmal stimuli.

To establish the role of complement activation we leveraged the differences in the AAA severity between *Apoe*$^{-/-}$ and AAV8-PCSK9/HFD models. We observed higher incidence of AAA dilatation, rupture, and death with Ang II infusion in *Mmp12*$^{-/-}$/*Apoe*$^{-/-}$ mice compared to *Mmp12*$^{-/-}$ mice on a high fat diet when injected with AAV8-PCSK9. Apo E is a glycoprotein component of several lipoprotein particles, which through binding to LDL receptors enables their hepatic clearance. Accordingly, Apo E deficiency leads to hyperlipidemia [55]. This mechanism of action is distinct from PCSK9, a serine protease that binds to hepatic LDL receptors and promotes their lysosomal degradation. Thus, similar to Apo E deficiency, adenovirus-mediated PCSK9 overexpression elevates plasma cholesterol levels in mice, a process that is enhanced with a high fat diet [55]. In addition to its effect on lipid metabolism, however, Apo E also impacts lipid peroxidation, inflammation, vascular smooth muscle cell proliferation and migration, and platelet aggregation [56–58]. As a result, *Apoe*$^{-/-}$ mice display a proinflammatory milieu [55], which may have contributed to the more severe phenotypes detected in these animals.

Normal arteries express low levels of MMP-12. To study the effect of macrophage MMP-12 in vascular remodeling, we relied on an inducible *Csf1r-Cre* system, which is classically used to target macrophages. The effect of the *Csf1r-iCre* system can also be detected in dendritic cells, granulocytes, and lymphocytes [59], yet, macrophages are classically considered the primary source of MMP-12 and MMP-12 expression is not detectable in normal blood cells [60–62]. Demonstration that macrophage MMP-12 is necessary for maintaining aortic wall integrity points to a new role for macrophages in regulating vascular homeostasis [63–65]. Future studies should establish whether activation of the complement system is systemic or local, and if so, which tissues are more susceptible to complement-mediated damage in the absence of MMP-12. The observation that a relatively short period of MMP-12-deficiency alters aortic integrity also raises the possibility that genetic and non-genetic factors that modulate MMP-12 expression may pre-dispose to AAA and other vascular pathologies. In this regard, it is noteworthy that polymorphisms in MMP-12 gene that reduce its level associate with higher predisposition to coronary artery disease and large artery atherosclerotic stroke [66].

In conclusion, this study suggests a novel role for macrophage MMP-12 in maintaining aortic integrity based on identification of an MMP-12 deficiency/complement activation/NETosis pathway that leads to adverse aortic remodeling and AAA rupture in multiple

mouse models. These findings also suggest caution in the use of selective MMP-12 inhibitors as therapeutic agents in AAA and other pathologies such as chronic obstructive pulmonary disease [67, 68]. Finally, considering these new findings, the role of MMP-12 in vascular homeostasis may mandate a re-evaluation of previous work on the roles of MMP-12 in various settings.

Supplementary Material

Refer to Web version on PubMed Central for supplementary material.

Sources of Funding

This work was supported by grants from NIH (R01 HL138567, R01 AG065917, U01 HL142518 and U54DK106857), Department of Veterans Affairs (I0-BX004038), and NIH T32 training grant (5T32HL007950). B.S. was supported by the European Union's Horizon 2020 research and innovation program (No. 793805) and the Netherlands Organization for Scientific Research (Rubicon 452172006). We acknowledge the assistance of the George M O'Brien Kidney Center at Yale (NIH grant P30 DK079310) for blood pressure measurements. We thank the Yale West Campus Imaging Core for the support and assistance in this work. We also thank Medical Research Council Harwell Institute, Mary Lyon Centre (UK) and INFRAFRONTIER/EMMA (www.infrafrontier.eu) for providing the mutant mouse line Mmp12tm1a(EUCOMM)Hmgu/H.

Non-standard Abbreviations and Acronyms

AAA	Abdominal aortic aneurysms
AAV8-PCSK9	Adeno-associated viral vector serotype 8 expressing gain-of-function proprotein convertase subtilisin/kexin type 9
AngII	Angiotensin II
BAPN	β-aminopropionitrile
C3	Complement component 3
C5a	Complement component 5a
Cit-H3	Citrullinated histone H3
DAPI	4′,6-diamidino-2-phenylindole
ECM	Extracellular matrix
HFD	High fat diet
IAA	Infrarenal abdominal aorta
IgG-FH$_{1–5}$	Factor H-Immunoglobulin G
MMP	Matrix metalloprotease
NE	Neutrophil elastase
NET	Neutrophil extracellular trap
R-CHP	Collagen Hybridizing Peptide, Cy3 Conjugate

SAA	Suprarenal abdominal aorta
SMA	Smooth muscle actin
VVG	Verhoeff-Van Gieson
WT	Wild-type

References

1. Ricklin D, Hajishengallis G, Yang K, Lambris JD. Complement: A key system for immune surveillance and homeostasis. Nat Immunol. 2010;11:785–797 [PubMed: 20720586]
2. Cosentino F, Lüscher TF. Maintenance of vascular integrity: Role of nitric oxide and other bradykinin mediators. Eur Heart J. 1995;16 Suppl K:4–12
3. Ho-Tin-Noé B, Boulaftali Y, Camerer E. Platelets and vascular integrity: How platelets prevent bleeding in inflammation. Blood. 2018;131:277–288 [PubMed: 29191915]
4. Halabi CM, Broekelmann TJ, Lin M, Lee VS, Chu ML, Mecham RP. Fibulin-4 is essential for maintaining arterial wall integrity in conduit but not muscular arteries. Sci Adv. 2017;3:e1602532 [PubMed: 28508064]
5. Döring Y, Noels H, van der Vorst EPC, Neideck C, Egea V, Drechsler M, Mandl M, Pawig L, Jansen Y, Schröder K, Bidzhekov K, Megens RTA, Theelen W, Klinkhammer BM, Boor P, Schurgers L, van Gorp R, Ries C, Kusters PJH, van der Wal A, Hackeng TM, Gäbel G, Brandes RP, Soehnlein O, Lutgens E, Vestweber D, Teupser D, Holdt LM, Rader DJ, Saleheen D, Weber C. Vascular cxcr4 limits atherosclerosis by maintaining arterial integrity: Evidence from mouse and human studies. Circulation. 2017;136:388–403 [PubMed: 28450349]
6. Slack MA, Gordon SM. Protease activity in vascular disease. Arteriosclerosis, thrombosis, and vascular biology. 2019;39:e210–e218 [PubMed: 31553665]
7. Curci JA, Liao S, Huffman MD, Shapiro SD, Thompson RW. Expression and localization of macrophage elastase (matrix metalloproteinase-12) in abdominal aortic aneurysms. J Clin Invest. 1998;102:1900–1910 [PubMed: 9835614]
8. Hellenthal FA, Buurman WA, Wodzig WK, Schurink GW. Biomarkers of aaa progression. Part 1: Extracellular matrix degeneration. Nat Rev Cardiol. 2009;6:464–474 [PubMed: 19468292]
9. Pyo R, Lee JK, Shipley JM, Curci JA, Mao D, Ziporin SJ, Ennis TL, Shapiro SD, Senior RM, Thompson RW. Targeted gene disruption of matrix metalloproteinase-9 (gelatinase b) suppresses development of experimental abdominal aortic aneurysms. J Clin Invest. 2000;105:1641–1649 [PubMed: 10841523]
10. Longo GM, Buda SJ, Fiotta N, Xiong W, Griener T, Shapiro S, Baxter BT. Mmp-12 has a role in abdominal aortic aneurysms in mice. Surgery. 2005;137:457–462 [PubMed: 15800495]
11. Wang Y, Ait-Oufella H, Herbin O, Bonnin P, Ramkhelawon B, Taleb S, Huang J, Offenstadt G, Combadiere C, Renia L, Johnson JL, Tharaux PL, Tedgui A, Mallat Z. Tgf-beta activity protects against inflammatory aortic aneurysm progression and complications in angiotensin ii-infused mice. J Clin Invest. 2010;120:422–432 [PubMed: 20101093]
12. Dean RA, Cox JH, Bellac CL, Doucet A, Starr AE, Overall CM. Macrophage-specific metalloelastase (mmp-12) truncates and inactivates elr+ cxc chemokines and generates ccl2, −7, −8, and −13 antagonists: Potential role of the macrophage in terminating polymorphonuclear leukocyte influx. Blood. 2008;112:3455–3464 [PubMed: 18660381]
13. Houghton AM, Hartzell WO, Robbins CS, Gomis-Ruth FX, Shapiro SD. Macrophage elastase kills bacteria within murine macrophages. Nature. 2009;460:637–641 [PubMed: 19536155]
14. Marchant DJ, Bellac CL, Moraes TJ, Wadsworth SJ, Dufour A, Butler GS, Bilawchuk LM, Hendry RG, Robertson AG, Cheung CT, Ng J, Ang L, Luo Z, Heilbron K, Norris MJ, Duan W, Bucyk T, Karpov A, Devel L, Georgiadis D, Hegele RG, Luo H, Granville DJ, Dive V, McManus BM, Overall CM. A new transcriptional role for matrix metalloproteinase-12 in antiviral immunity. Nat Med. 2014;20:493–502 [PubMed: 24784232]

15. Liu Y, Zhang M, Hao W, Mihaljevic I, Liu X, Xie K, Walter S, Fassbender K. Matrix metalloproteinase-12 contributes to neuroinflammation in the aged brain. Neurobiol Aging. 2013;34:1231–1239 [PubMed: 23159549]

16. Iyer RP, Patterson NL, Zouein FA, Ma Y, Dive V, de Castro Bras LE, Lindsey ML. Early matrix metalloproteinase-12 inhibition worsens post-myocardial infarction cardiac dysfunction by delaying inflammation resolution. Int J Cardiol. 2015;185:198–208 [PubMed: 25797678]

17. Johnson JL, Devel L, Czarny B, George SJ, Jackson CL, Rogakos V, Beau F, Yiotakis A, Newby AC, Dive V. A selective matrix metalloproteinase-12 inhibitor retards atherosclerotic plaque development in apolipoprotein e-knockout mice. Arterioscler Thromb Vasc Biol. 2011;31:528–535 [PubMed: 21212406]

18. Razavian M, Bordenave T, Georgiadis D, Beau F, Zhang J, Golestani R, Toczek J, Jung JJ, Ye Y, Kim HY, Han J, Dive V, Devel L, Sadeghi MM. Optical imaging of mmp-12 active form in inflammation and aneurysm. Sci Rep. 2016;6:38345 [PubMed: 27917892]

19. Daugherty A, Manning MW, Cassis LA. Angiotensin ii promotes atherosclerotic lesions and aneurysms in apolipoprotein e-deficient mice. J Clin Invest. 2000;105:1605–1612 [PubMed: 10841519]

20. Aryal B, Singh AK, Zhang X, Varela L, Rotllan N, Goedeke L, Chaube B, Camporez JP, Vatner DF, Horvath TL, Shulman GI, Suarez Y, Fernandez-Hernando C. Absence of angptl4 in adipose tissue improves glucose tolerance and attenuates atherogenesis. JCI Insight. 2018;3

21. Lu G, Su G, Davis JP, Schaheen B, Downs E, Roy RJ, Ailawadi G, Upchurch GR Jr. A novel chronic advanced stage abdominal aortic aneurysm murine model. J Vasc Surg. 2017;66:232–242 e234 [PubMed: 28274752]

22. Shipley JM, Wesselschmidt RL, Kobayashi DK, Ley TJ, Shapiro SD. Metalloelastase is required for macrophage-mediated proteolysis and matrix invasion in mice. Proc Natl Acad Sci U S A. 1996;93:3942–3946 [PubMed: 8632994]

23. Qian BZ, Li J, Zhang H, Kitamura T, Zhang J, Campion LR, Kaiser EA, Snyder LA, Pollard JW. Ccl2 recruits inflammatory monocytes to facilitate breast-tumour metastasis. Nature. 2011;475:222–225 [PubMed: 21654748]

24. Ricard N, Scott RP, Booth CJ, Velazquez H, Cilfone NA, Baylon JL, Gulcher JR, Quaggin SE, Chittenden TW, Simons M. Endothelial erk1/2 signaling maintains integrity of the quiescent endothelium. J Exp Med. 2019;216:1874–1890 [PubMed: 31196980]

25. Zhang X, Goncalves R, Mosser DM. The isolation and characterization of murine macrophages. Curr Protoc Immunol. 2008;Chapter 14:Unit 14 11

26. Gleason RL, Gray SP, Wilson E, Humphrey JD. A multiaxial computer-controlled organ culture and biomechanical device for mouse carotid arteries. J Biomech Eng. 2004;126:787–795 [PubMed: 15796337]

27. Ferruzzi J, Bersi MR, Humphrey JD. Biomechanical phenotyping of central arteries in health and disease: Advantages of and methods for murine models. Ann Biomed Eng. 2013;41:1311–1330 [PubMed: 23549898]

28. Kawamura Y, Murtada SI, Gao F, Liu X, Tellides G, Humphrey JD. Adventitial remodeling protects against aortic rupture following late smooth muscle-specific disruption of tgfbeta signaling. J Mech Behav Biomed Mater. 2021;116:104264 [PubMed: 33508556]

29. Toczek J, Boodagh P, Sanzida N, Ghim M, Salarian M, Gona K, Kukreja G, Rajendran S, Wei L, Han J, Zhang J, Jung JJ, Graham M, Liu X, Sadeghi MM. Computed tomography imaging of macrophage phagocytic activity in abdominal aortic aneurysm. Theranostics. 2021;11:5876–5888 [PubMed: 33897887]

30. Cao RY, Amand T, Ford MD, Piomelli U, Funk CD. The murine angiotensin ii-induced abdominal aortic aneurysm model: Rupture risk and inflammatory progression patterns. Front Pharmacol. 2010;1:9 [PubMed: 21713101]

31. Golledge J. Abdominal aortic aneurysm: Update on pathogenesis and medical treatments. Nat Rev Cardiol. 2019;16:225–242 [PubMed: 30443031]

32. Bjorklund MM, Hollensen AK, Hagensen MK, Dagnaes-Hansen F, Christoffersen C, Mikkelsen JG, Bentzon JF. Induction of atherosclerosis in mice and hamsters without germline genetic engineering. Circ Res. 2014;114:1684–1689 [PubMed: 24677271]

33. Jana S, Hu M, Shen M, Kassiri Z. Extracellular matrix, regional heterogeneity of the aorta, and aortic aneurysm. Exp Mol Med. 2019;51:1–15
34. de Bont CM, Boelens WC, Pruijn GJM. Netosis, complement, and coagulation: A triangular relationship. Cell Mol Immunol. 2019;16:19–27 [PubMed: 29572545]
35. Zelek WM, Morgan BP. Monoclonal antibodies capable of inhibiting complement downstream of c5 in multiple species. Front Immunol. 2020;11:612402 [PubMed: 33424866]
36. Gilmore AC, Zhang Y, Cook HT, Lavin DP, Katti S, Wang Y, Johnson KK, Kim S, Pickering MC. Complement activity is regulated in c3 glomerulopathy by igg-factor h fusion proteins with and without properdin targeting domains. Kidney Int. 2021;99:396–404 [PubMed: 33129896]
37. Quintana RA, Taylor WR. Cellular mechanisms of aortic aneurysm formation. Circ Res. 2019;124:607–618 [PubMed: 30763207]
38. Spronck B, Latorre M, Wang M, Mehta S, Caulk AW, Ren P, Ramachandra AB, Murtada SI, Rojas A, He CS, Jiang B, Bersi MR, Tellides G, Humphrey JD. Excessive adventitial stress drives inflammation-mediated fibrosis in hypertensive aortic remodelling in mice. J R Soc Interface. 2021;18:20210336 [PubMed: 34314650]
39. Shen M, Lee J, Basu R, Sakamuri SS, Wang X, Fan D, Kassiri Z. Divergent roles of matrix metalloproteinase 2 in pathogenesis of thoracic aortic aneurysm. Arterioscler Thromb Vasc Biol. 2015;35:888–898 [PubMed: 25657308]
40. Howatt DA, Dajee M, Xie X, Moorleghen J, Rateri DL, Balakrishnan A, Da Cunha V, Johns DG, Gutstein DE, Daugherty A, Lu H. Relaxin and matrix metalloproteinase-9 in angiotensin ii-induced abdominal aortic aneurysms. Circ J. 2017;81:888–890 [PubMed: 28420827]
41. Longo GM, Xiong W, Greiner TC, Zhao Y, Fiotti N, Baxter BT. Matrix metalloproteinases 2 and 9 work in concert to produce aortic aneurysms. J Clin Invest. 2002;110:625–632 [PubMed: 12208863]
42. Deguchi JO, Huang H, Libby P, Aikawa E, Whittaker P, Sylvan J, Lee RT, Aikawa M. Genetically engineered resistance for mmp collagenases promotes abdominal aortic aneurysm formation in mice infused with angiotensin ii. Lab Invest. 2009;89:315–326 [PubMed: 19153555]
43. Rosell A, Lo EH. Multiphasic roles for matrix metalloproteinases after stroke. Curr Opin Pharmacol. 2008;8:82–89 [PubMed: 18226583]
44. Bellac CL, Dufour A, Krisinger MJ, Loonchanta A, Starr AE, Auf dem Keller U, Lange PF, Goebeler V, Kappelhoff R, Butler GS, Burtnick LD, Conway EM, Roberts CR, Overall CM. Macrophage matrix metalloproteinase-12 dampens inflammation and neutrophil influx in arthritis. Cell Rep. 2014;9:618–632 [PubMed: 25310974]
45. Dufour A, Bellac CL, Eckhard U, Solis N, Klein T, Kappelhoff R, Fortelny N, Jobin P, Rozmus J, Mark J, Pavlidis P, Dive V, Barbour SJ, Overall CM. C-terminal truncation of ifn-gamma inhibits proinflammatory macrophage responses and is deficient in autoimmune disease. Nat Commun. 2018;9:2416 [PubMed: 29925830]
46. Merle NS, Church SE, Fremeaux-Bacchi V, Roumenina LT. Complement system part i - molecular mechanisms of activation and regulation. Front Immunol. 2015;6:262 [PubMed: 26082779]
47. Xie CB, Jane-Wit D, Pober JS. Complement membrane attack complex: New roles, mechanisms of action, and therapeutic targets. Am J Pathol. 2020;190:1138–1150 [PubMed: 32194049]
48. Martin-Ventura JL, Martinez-Lopez D, Roldan-Montero R, Gomez-Guerrero C, Blanco-Colio LM. Role of complement system in pathological remodeling of the vascular wall. Mol Immunol. 2019;114:207–215 [PubMed: 31377677]
49. Zhou HF, Yan H, Stover CM, Fernandez TM, Rodriguez de Cordoba S, Song WC, Wu X, Thompson RW, Schwaeble WJ, Atkinson JP, Hourcade DE, Pham CT. Antibody directs properdin-dependent activation of the complement alternative pathway in a mouse model of abdominal aortic aneurysm. Proc Natl Acad Sci U S A. 2012;109:E415–422 [PubMed: 22308431]
50. Papayannopoulos V. Neutrophil extracellular traps in immunity and disease. Nat Rev Immunol. 2018;18:134–147 [PubMed: 28990587]
51. Yan H, Zhou HF, Akk A, Hu Y, Springer LE, Ennis TL, Pham CTN. Neutrophil proteases promote experimental abdominal aortic aneurysm via extracellular trap release and plasmacytoid dendritic cell activation. Arterioscler Thromb Vasc Biol. 2016;36:1660–1669 [PubMed: 27283739]

52. Meher AK, Spinosa M, Davis JP, Pope N, Laubach VE, Su G, Serbulea V, Leitinger N, Ailawadi G, Upchurch GR Jr. Novel role of il (interleukin)-1beta in neutrophil extracellular trap formation and abdominal aortic aneurysms. Arterioscler Thromb Vasc Biol. 2018;38:843–853 [PubMed: 29472233]

53. Rateri DL, Davis FM, Balakrishnan A, Howatt DA, Moorleghen JJ, O'Connor WN, Charnigo R, Cassis LA, Daugherty A. Angiotensin ii induces region-specific medial disruption during evolution of ascending aortic aneurysms. Am J Pathol. 2014;184:2586–2595 [PubMed: 25038458]

54. Luo W, Wang Y, Zhang L, Ren P, Zhang C, Li Y, Azares AR, Zhang M, Guo J, Ghaghada KB, Starosolski ZA, Rajapakshe K, Coarfa C, Li Y, Chen R, Fujiwara K, Abe JI, Coselli JS, Milewicz DM, LeMaire SA, Shen YH. Critical role of cytosolic DNA and its sensing adaptor sting in aortic degeneration, dissection, and rupture. Circulation. 2020;141:42–66 [PubMed: 31887080]

55. Emini Veseli B, Perrotta P, De Meyer GRA, Roth L, Van der Donckt C, Martinet W, De Meyer GRY. Animal models of atherosclerosis. Eur J Pharmacol. 2017;816:3–13 [PubMed: 28483459]

56. Hayek T, Oiknine J, Brook JG, Aviram M. Increased plasma and lipoprotein lipid peroxidation in apo e-deficient mice. Biochem Biophys Res Commun. 1994;201:1567–1574 [PubMed: 8024602]

57. Hui DY, Basford JE. Distinct signaling mechanisms for apoe inhibition of cell migration and proliferation. Neurobiol Aging. 2005;26:317–323 [PubMed: 15639309]

58. Riddell DR, Graham A, Owen JS. Apolipoprotein e inhibits platelet aggregation through the l-arginine:Nitric oxide pathway. Implications for vascular disease. J Biol Chem. 1997;272:89–95 [PubMed: 8995232]

59. McCubbrey AL, Allison KC, Lee-Sherick AB, Jakubzick CV, Janssen WJ. Promoter specificity and efficacy in conditional and inducible transgenic targeting of lung macrophages. Front Immunol. 2017;8:1618 [PubMed: 29225599]

60. Thul PJ, Akesson L, Wiking M, Mahdessian D, Geladaki A, Ait Blal H, Alm T, Asplund A, Bjork L, Breckels LM, Backstrom A, Danielsson F, Fagerberg L, Fall J, Gatto L, Gnann C, Hober S, Hjelmare M, Johansson F, Lee S, Lindskog C, Mulder J, Mulvey CM, Nilsson P, Oksvold P, Rockberg J, Schutten R, Schwenk JM, Sivertsson A, Sjostedt E, Skogs M, Stadler C, Sullivan DP, Tegel H, Winsnes C, Zhang C, Zwahlen M, Mardinoglu A, Ponten F, von Feilitzen K, Lilley KS, Uhlen M, Lundberg E. A subcellular map of the human proteome. Science. 2017;356

61. Uhlen M, Fagerberg L, Hallstrom BM, Lindskog C, Oksvold P, Mardinoglu A, Sivertsson A, Kampf C, Sjostedt E, Asplund A, Olsson I, Edlund K, Lundberg E, Navani S, Szigyarto CA, Odeberg J, Djureinovic D, Takanen JO, Hober S, Alm T, Edqvist PH, Berling H, Tegel H, Mulder J, Rockberg J, Nilsson P, Schwenk JM, Hamsten M, von Feilitzen K, Forsberg M, Persson L, Johansson F, Zwahlen M, von Heijne G, Nielsen J, Ponten F. Proteomics. Tissue-based map of the human proteome. Science. 2015;347:1260419 [PubMed: 25613900]

62. Andersen HR, Maeng M, Thorwest M, Falk E. Remodeling rather than neointimal formation explains luminal narrowing after deep vessel wall injury: Insights from a porcine coronary (re)stenosis model. Circulation. 1996;93:1716–1724 [PubMed: 8653878]

63. Okabe Y, Medzhitov R. Tissue biology perspective on macrophages. Nat Immunol. 2016;17:9–17 [PubMed: 26681457]

64. Wynn TA, Chawla A, Pollard JW. Macrophage biology in development, homeostasis and disease. Nature. 2013;496:445–455 [PubMed: 23619691]

65. Watanabe S, Alexander M, Misharin AV, Budinger GRS. The role of macrophages in the resolution of inflammation. J Clin Invest. 2019;129:2619–2628 [PubMed: 31107246]

66. Sun BB, Maranville JC, Peters JE, Stacey D, Staley JR, Blackshaw J, Burgess S, Jiang T, Paige E, Surendran P, Oliver-Williams C, Kamat MA, Prins BP, Wilcox SK, Zimmerman ES, Chi A, Bansal N, Spain SL, Wood AM, Morrell NW, Bradley JR, Janjic N, Roberts DJ, Ouwehand WH, Todd JA, Soranzo N, Suhre K, Paul DS, Fox CS, Plenge RM, Danesh J, Runz H, Butterworth AS. Genomic atlas of the human plasma proteome. Nature. 2018;558:73–79 [PubMed: 29875488]

67. Devel L, Rogakos V, David A, Makaritis A, Beau F, Cuniasse P, Yiotakis A, Dive V. Development of selective inhibitors and substrate of matrix metalloproteinase-12. J Biol Chem. 2006;281:11152–11160 [PubMed: 16481329]

68. Toczek J, Bordenave T, Gona K, Kim HY, Beau F, Georgiadis D, Correia I, Ye Y, Razavian M, Jung JJ, Lequin O, Dive V, Sadeghi MM, Devel L. Novel matrix metalloproteinase 12

selective radiotracers for vascular molecular imaging. J Med Chem. 2019;62:9743–9752 [PubMed: 31603669]

Novelty and Significance

What Is known?

- Extracellular matrix and matricellular components of the vascular wall play important roles in maintaining integrity and normal function of the arterial wall.
- Matrix metalloproteinase-12 (MMP-12 or macrophage elastase) is highly upregulated in abdominal aortic aneurysms (AAA) in humans and multiple mouse models.
- Degradation of elastic fibers is a key component of AAA pathogenesis, and MMP-12 is generally considered to play a major role in this process.

What New Information Does This Article Contribute?

- MMP-12 deficiency leads to activation of the complement system and neutrophil extracellular trap formation and predisposes the aorta to AAA development and rupture.
- Macrophage MMP-12 is essential for aortic homeostasis and integrity.

There is conflicting information on the role MMP-12, a highly upregulated elastase, in AAA development. Here, we demonstrate that MMP-12 is crucial for maintaining vascular homeostasis, and MMP-12 deficiency results in complement activation and elevated levels of neutrophil extracellular traps along the aorta, increasing the susceptibility to AAA and its rupture. These findings suggest caution in the use of selective MMP-12 inhibitors as therapeutic agents in AAA and mandate a re-evaluation of previous work on the roles of MMP-12 in various settings.

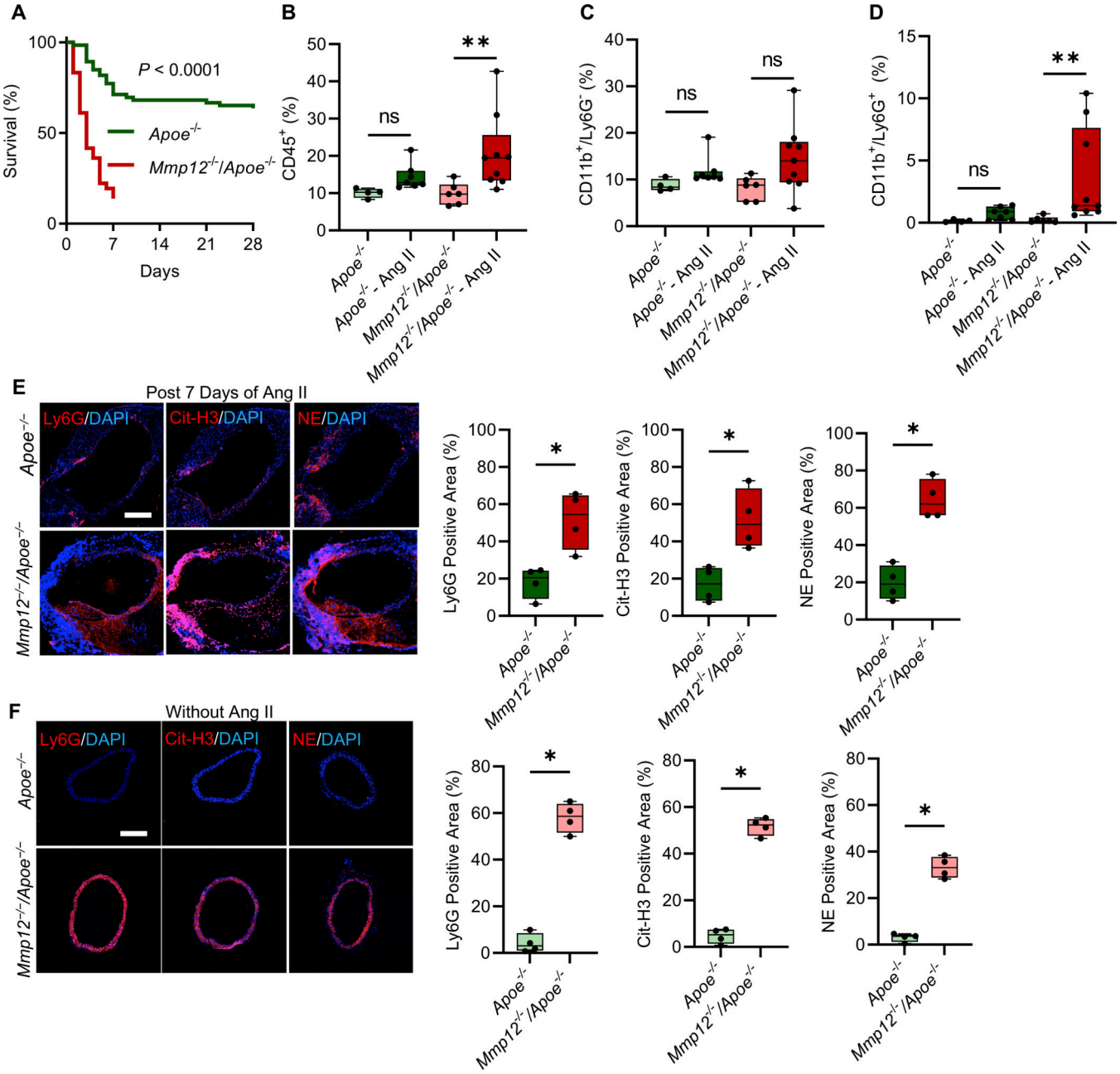

Figure 1. Effect of *Mmp12* deletion on AngII-induced AAA development and progression in *Apoe*$^{-/-}$ mice.

A. Kaplan-Meier survival curves of AngII-induced AAA in *Apoe*$^{-/-}$ (n = 66) and *Mmp12*$^{-/-}$/*Apoe*$^{-/-}$ (n = 36) mice. The curves were compared using Log-rank (Mantel-Cox) test. $P < 0.0001$. **B-D.** Flow cytometric evaluation of CD45^{+} cells (**B**), CD11b^{+}/Ly6G^{-} mononuclear myeloid cells, primarily macrophages (**C**), and CD11b^{+}/Ly6G^{+} neutrophils (**D**) as % among live cells in aortas of *Apoe*$^{-/-}$ and *Mmp12*$^{-/-}$/*Apoe*$^{-/-}$ mice after 18–24 h of AngII or saline (control) infusion. Values are expressed as means ± SD; n = 4 to 9 per group, ns: not significant. **E, F.** Representative images of immunofluorescence staining and quantification of neutrophils (Ly6G, red), neutrophil extracellular traps (Cit-H3, red),

and NE (red) in surviving *Apoe*$^{-/-}$ and *Mmp12*$^{-/-}$/*Apoe*$^{-/-}$ mice after 7 days of AngII infusion (**E**) and control animals (**F**). Nuclei are stained blue with DAPI. n = 4 per group. Scale bar: 500 μm. Cit-H3: citrullinated histone 3, NE: neutrophil elastase. *$P < 0.05$ by Kruskal-Wallis with Dunn's multiple comparisons post hoc test (**B-D**) or by two-tailed Mann-Whitney U test (**E, F**).

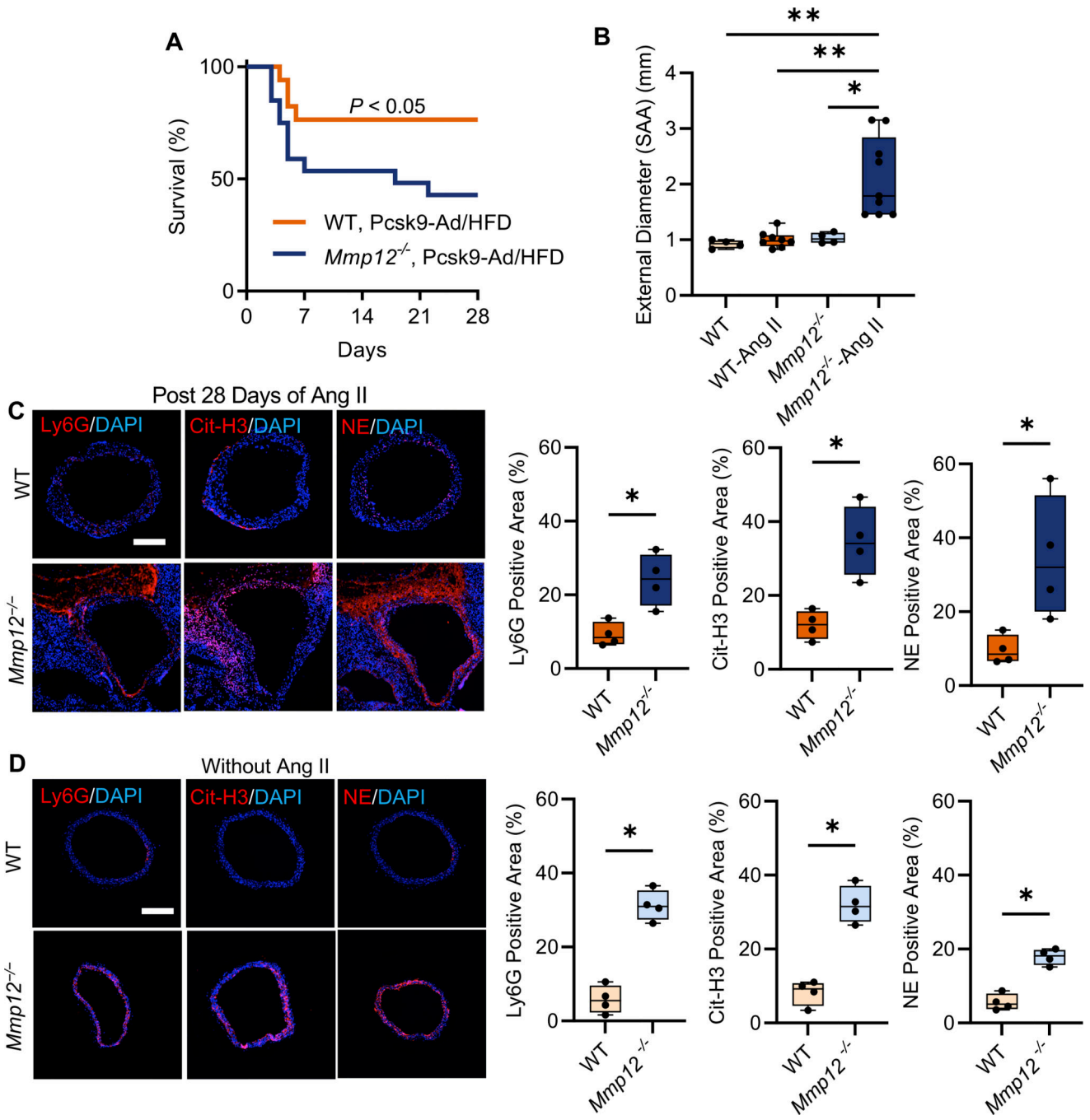

Figure 2. Effect of *Mmp12* deletion on AngII-induced AAA development and progression in hyperlipidemic WT mice.

A. Kaplan-Meier survival curves of AngII-induced AAA in hyperlipidemic WT (n = 17) and *Mmp12*$^{-/-}$ (n = 20) mice. The curves were compared using Log-rank (Mantel-Cox) test. $P < 0.05$. **B**. Quantification of maximal suprarenal abdominal aorta external diameter at baseline (no AngII) and in animals surviving 4 weeks of AngII infusion; n = 4 to 9. **C, D.** Representative immunofluorescence staining images and quantification of neutrophils (Ly6G, red), neutrophil extracellular traps (Cit-H3, red), and NE (red) in

surviving hyperlipidemic WT and *Mmp12*$^{-/-}$ mice after 28 days of AngII infusion (**C**) and saline-infused control animals (**D**). Nuclei are stained blue with DAPI. n = 4 per group. Scale bar: 500 μm. WT: hyperlipidemic wild type, Cit-H3: citrullinated histone 3, NE: neutrophil elastase. *$P < 0.05$, **$P < 0.01$, by Kruskal-Wallis test with Dunn's multiple comparisons post hoc test (**B**), or *$P < 0.05$, by two-tailed Mann-Whitney U test (**C, D**).

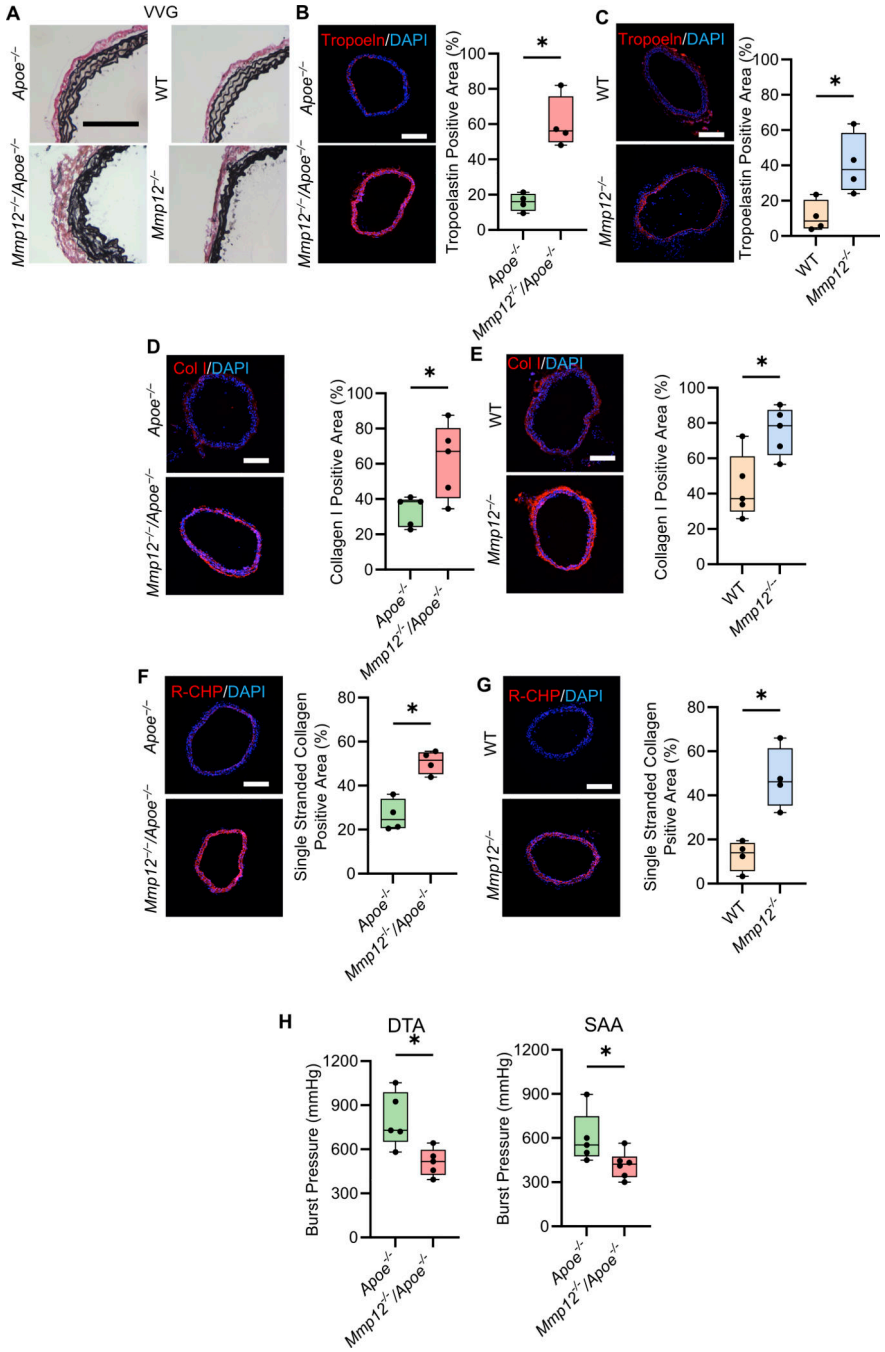

Figure 3. Effect of *Mmp12* deficiency on aortic wall extracellular matrix composition.

A. Representative examples of Verhoeff–van Gieson (VVG) staining of suprarenal abdominal aorta in *Apoe*$^{-/-}$ and *Mmp12*$^{-/-}$/*Apoe*$^{-/-}$ (left column) and wild type (WT) and *Mmp12*$^{-/-}$ (right column) mice. Scale bar: 250 μm. **B-G.** Representative images of immunofluorescence staining and quantification of tropoelastin (red, panels **B** and **C**), collagen type I (red, panels **D** and **E**) and single stranded collagen using collagen hybridizing peptide, Cy3 conjugate (R-CHP) (red, panels **F** and **G**) in *Apoe*$^{-/-}$ and *Mmp12*$^{-/-}$/*Apoe*$^{-/-}$ (panels **B**, **D**, and **F**) and WT and *Mmp12*$^{-/-}$ (panels **C**, **E**, and **G**)

mice. Nuclei are stained blue with DAPI. n = 4 per group. Scale bar: 500 μm. **H.** Burst pressure, as a functional readout of wall strength, of descending thoracic aorta (DTA) and suprarenal abdominal aorta (SAA) in *Apoe*$^{-/-}$ and *Mmp12*$^{-/-}$/*Apoe*$^{-/-}$ mice. n = 5 to 6 per group. **P* < 0.05, ***P* < 0.01 by two-tailed Mann-Whitney U test (**B**-**H**).

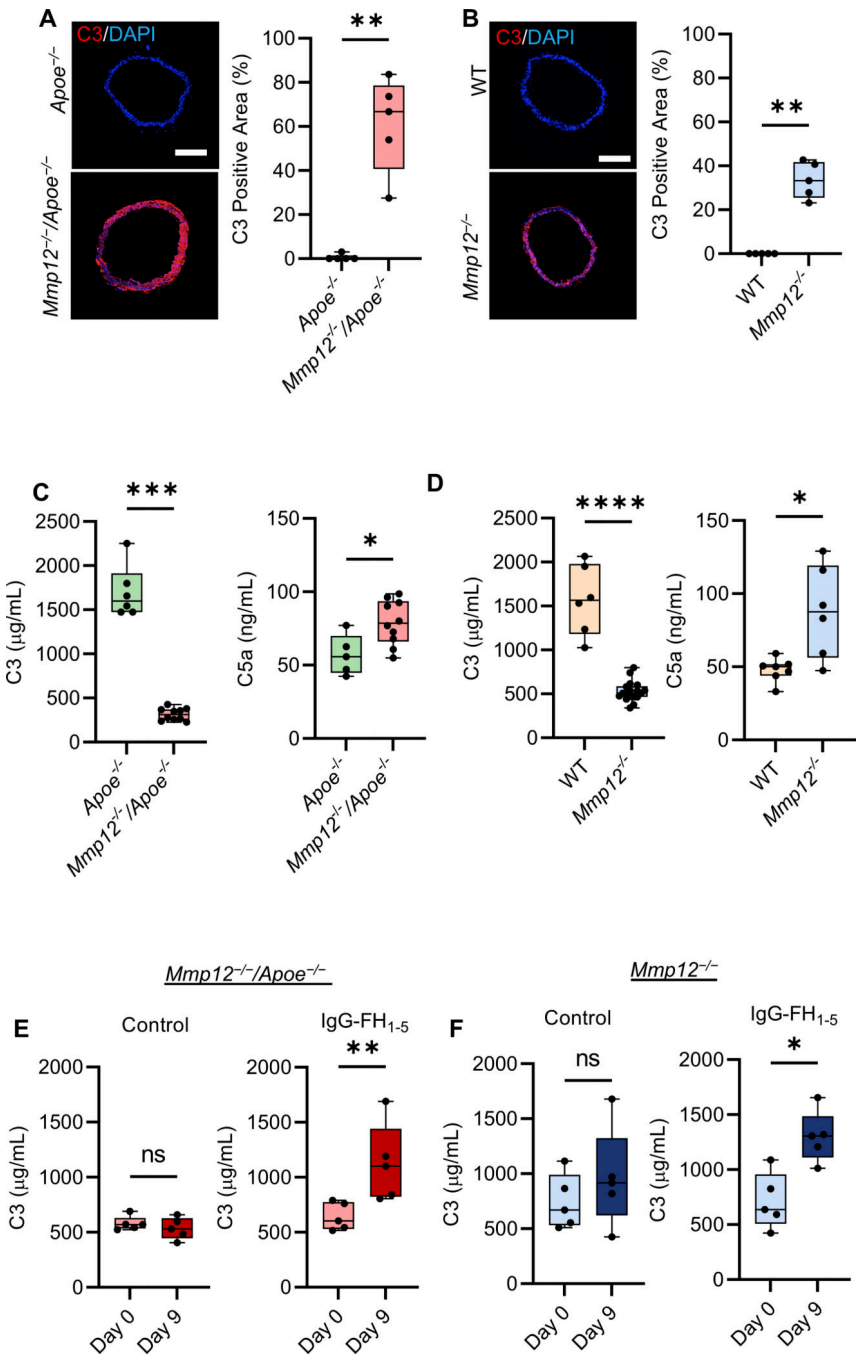

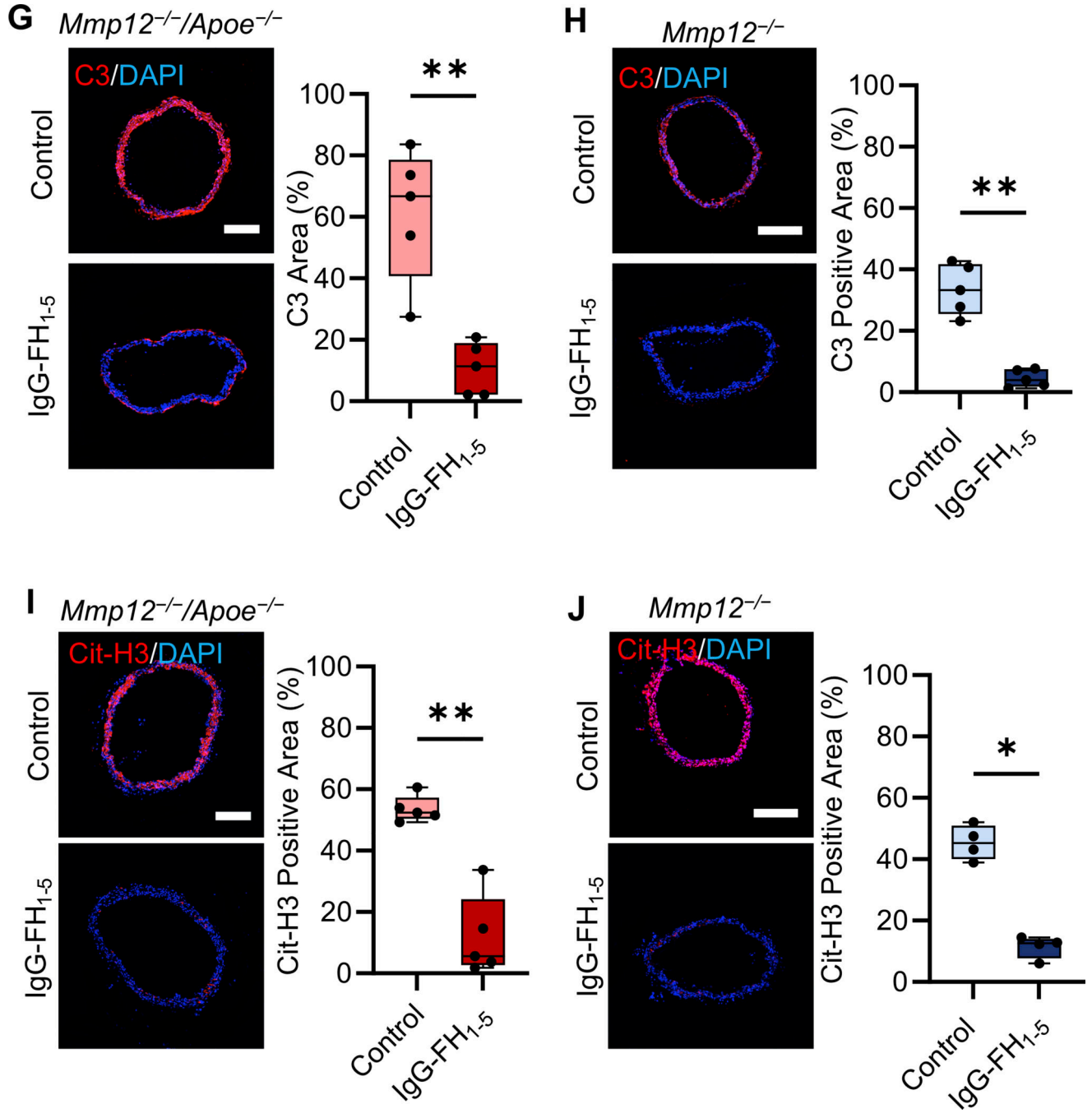

Figure 4. Effect of *Mmp12* deletion on aortic wall complement deposition.

A, B. Representative images of immunofluorescence staining and quantification of C3 deposits (red) in suprarenal abdominal aorta of *Apoe*$^{-/-}$ and *Mmp12*$^{-/-}$/*Apoe*$^{-/-}$ (**A**), and wild type (WT) and *Mmp12*$^{-/-}$ (**B**) mice. Nuclei are stained with DAPI in blue. n = 5 per group. Scale bar: 500 μm. **C, D.** Plasma C3 and C5a levels of *Apoe*$^{-/-}$ and *Mmp12*$^{-/-}$/*Apoe*$^{-/-}$ (**C**), and WT and *Mmp12*$^{-/-}$ (**D**) mice. n = 5 to 10 per group. **E, F.** Plasma C3 levels in *Mmp12*$^{-/-}$/*Apoe*$^{-/-}$ (**E**) and *Mmp12*$^{-/-}$ (**F**) mice at baseline and 9 days of treatment with IgG-FH$_{1–5}$ or MOPC antibody (control). n = 5 per group. **G, H.** Representative images

of immunofluorescence staining and quantification of C3 (red) in suprarenal abdominal aorta of *Mmp12*$^{-/-}$/*Apoe*$^{-/-}$ (**G**) and *Mmp12*$^{-/-}$ (**H**) mice after 9 days of treatment with IgG-FH$_{1–5}$ or MOPC antibody (control). n = 5 per group; Scale bar: 500 μm**. I, J.** Representative images of immunofluorescence staining and quantification of Cit-H3 (red) in suprarenal abdominal aorta of *Mmp12*$^{-/-}$/*Apoe*$^{-/-}$ (**I**) and *Mmp12*$^{-/-}$ (**J**) mice after 9 days of treatment with IgG-FH$_{1–5}$ or MOPC antibody (control). n = 4 to 5 per group. Scale bar: 500 μm. **P* < 0.05, ***P* < 0.01, *****P* < 0.0001 by two-tailed Mann-Whitney U test (**A**-**J**).

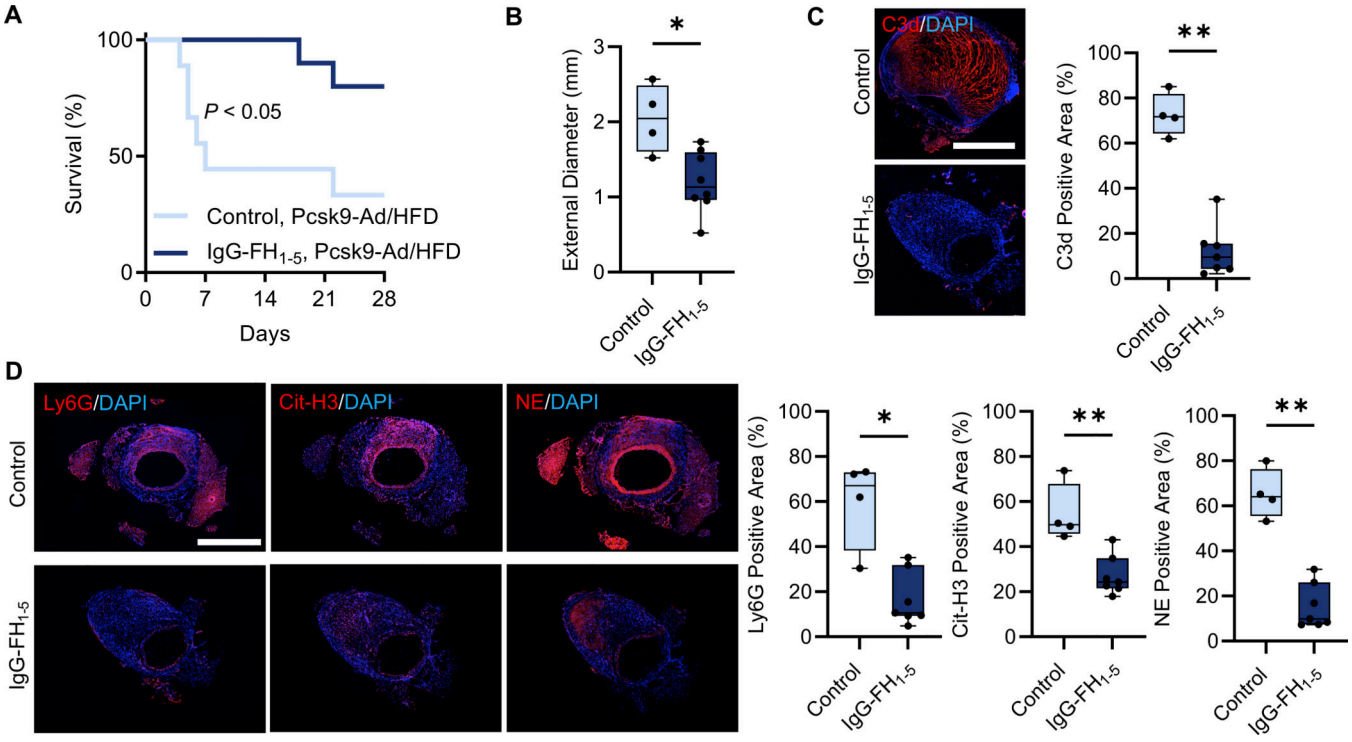

Figure 5. Effect of IgG-FH$_{1–5}$ on survival during AngII infusion in *Mmp12*$^{-/-}$ mice.

A. Kaplan-Meier survival curves of AngII-infused *Mmp12*$^{-/-}$ mice following Pcsk9-Ad injection and high fat diet (HFD), treated with either IgG-FH$_{1–5}$ or MOPC antibody as control (n = 10 per group). The curves were compared using Log-rank (Mantel-Cox) test, $P < 0.05$. **B.** Quantification of maximal suprarenal abdominal aorta external diameter after 4 weeks of AngII infusion in surviving *Mmp12*$^{-/-}$ mice treated with either IgG-FH$_{1–5}$ or MOPC antibody, n = 4 to 8 per group. **C.** Representative images of immunofluorescence staining and quantification of complement component 3d (C3d, red) deposition in suprarenal abdominal aorta of surviving IgG-FH$_{1–5}$- or MOPC-treated *Mmp12*$^{-/-}$ mice after 28 days of AngII infusion. Nuclei are stained blue with DAPI. n = 4 to 7 per group; Scale bar: 500 μm. **D.** Representative images of immunofluorescence staining and quantification of neutrophils (Ly6G, red), NETs (Cit-H3, red), and NE (red) in suprarenal abdominal aorta of surviving IgG-FH$_{1–5}$- or MOPC-treated *Mmp12*$^{-/-}$ mice after 28 days of AngII infusion. Nuclei are stained blue with DAPI. n = 4 to 7 per group; Scale bar: 500 μm. NET: neutrophil extracellular trap, Cit-H3: citrullinated histone 3, NE: neutrophil elastase. *$P < 0.05$, **$P < 0.01$ by two-tailed Mann-Whitney U test (**B-D**).

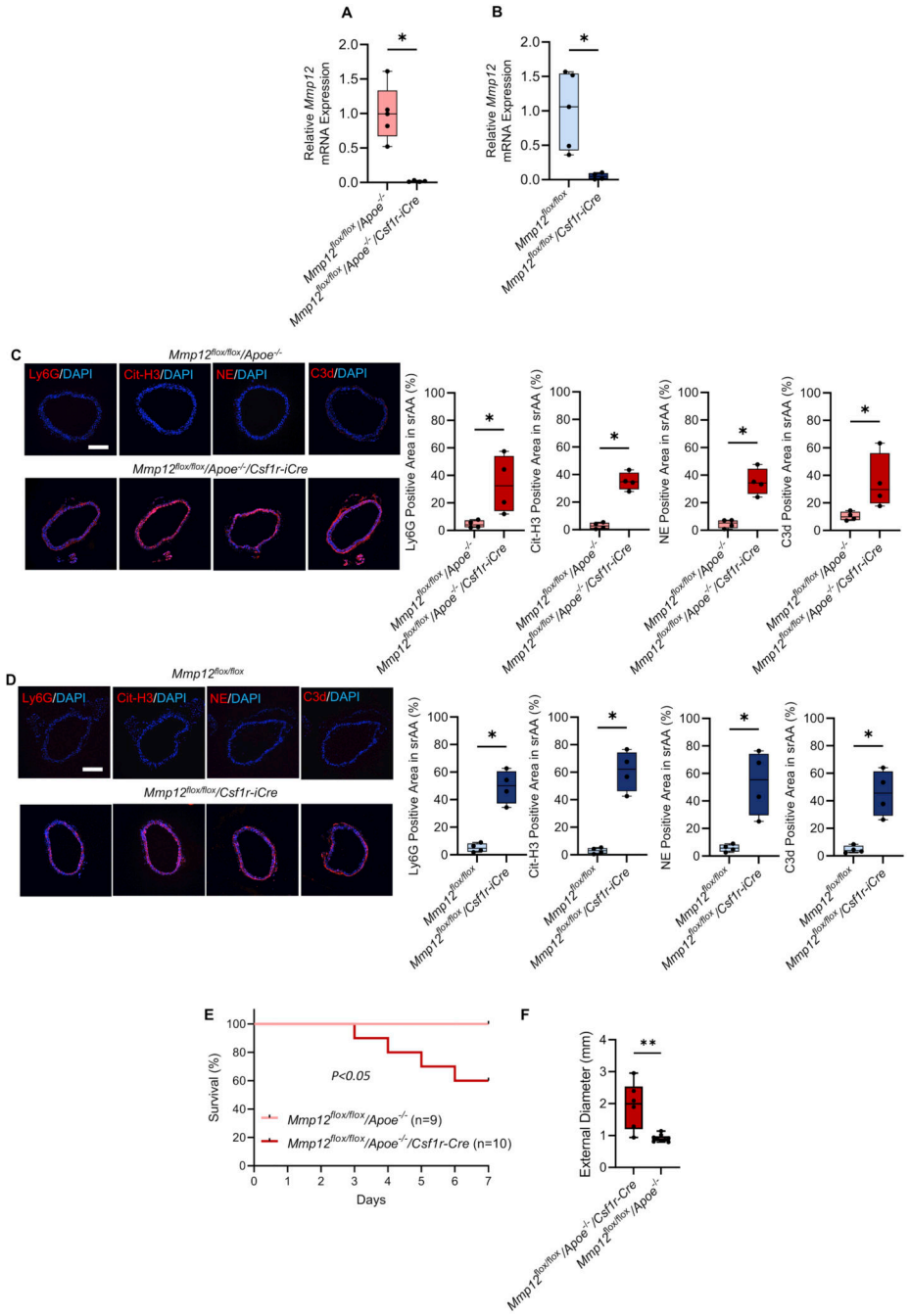

Figure 6. Effect of macrophage *Mmp12* deficiency on aortic composition and AngII-induced AAA development and survival.

A, B. Relative β-actin-normalized *Mmp12* gene expression in bone-marrow-derived macrophages from *Mmp12*$^{flox/flox}$/*Apoe*$^{-/-}$ and *Mmp12*$^{flox/flox}$/*Apoe*$^{-/-}$/*Csf1r-iCre* (**A**), and *Mmp12*$^{flox/flox}$ and *Mmp12*$^{flox/flox}$/*Csf1r-iCre* (**B**) mice at 5–6 weeks post-tamoxifen administration. n = 4 to 5 per group; * $P < 0.05$. **C, D.** Representative images of immunofluorescence staining and quantification of Neutrophils (Ly6G, red), NETs (Cit-H3, red), and complement component 3d (C3d, red) in suprarenal abdominal aorta of

Mmp12$^{flox/flox}$/*Apoe*$^{-/-}$ and *Mmp12*$^{flox/flox}$/*Apoe*$^{-/-}$/*Csf1r-iCre* (**C**) and *Mmp12*$^{flox/flox}$ and *Mmp12*$^{flox/flox}$/*Csf1r-iCre* (**D**) mice at 5–6 weeks post-tamoxifen administration. Nuclei are stained blue with DAPI. n = 4 per group. Scale bar: 500 μm. *$P < 0.05$, two-tailed Mann-Whitney U test (**A**-**D**). **E**. Kaplan-Meier survival curves of AngII-infused *Mmp12* $^{flox/flox}$/*Apoe*$^{-/-}$ (n=9) and *Mmp12* $^{flox/flox}$/*Apoe*$^{-/-}$/*Csf1r-iCre* (n=10) mice post-tamoxifen administration. The curves were compared using Log-rank (Mantel-Cox) test. $P < 0.05$. **F**. Quantification of maximal suprarenal abdominal aorta external diameter of the surviving mice. **$P < 0.01$ by two-tailed Mann-Whitney U test.